Calhoun: The NPS Institutional Archive

DSpace Repository

Theses and Dissertations | 1. Thesis and Dissertation Collection, all items

1994-12

Modal analysis of the PHALANX M61A1 close-in weapons system

Hansberry, Robert J.

Monterey, California. Naval Postgraduate School

http://hdl.handle.net/10945/42812

This publication is a work of the U.S. Government as defined in Title 17, United States Code, Section 101. Copyright protection is not available for this work in the United States.

Downloaded from NPS Archive: Calhoun

http://www.nps.edu/library

Calhoun is the Naval Postgraduate School's public access digital repository for research materials and institutional publications created by the NPS community. Calhoun is named for Professor of Mathematics Guy K. Calhoun, NPS's first appointed -- and published -- scholarly author.

Dudley Knox Library / Naval Postgraduate School
411 Dyer Road / 1 University Circle
Monterey, California USA 93943

NAVAL POSTGRADUATE SCHOOL
MONTEREY, CALIFORNIA

DTIC
ELECTE
APR 17 1995
S D
B

THESIS

MODAL ANALYSIS OF THE PHALANX M61A1 CLOSE-IN WEAPONS SYSTEM

by

Robert J. Hansberry

December, 1994

Thesis Advisor: Steven R. Baker
Second Reader: Robert M. Keolian

Approved for public release; distribution is unlimited.

19950414 072

DTIC QUALITY INSPECTED 5

REPORT DOCUMENTATION PAGE

Form Approved OMB No. 0704-0188

Public reporting burden for this collection of information is estimated to average 1 hour per response, including the time for reviewing instruction, searching existing data sources, gathering and maintaining the data needed, and completing and reviewing the collection of information. Send comments regarding this burden estimate or any other aspect of this collection of information, including suggestions for reducing this burden, to Washington Headquarters Services, Directorate for Information Operations and Reports, 1215 Jefferson Davis Highway, Suite 1204, Arlington, VA 22202-4302, and to the Office of Management and Budget, Paperwork Reduction Project (0704-0188) Washington DC 20503.

1. AGENCY USE ONLY *(Leave blank)*	2. REPORT DATE December 94	3. REPORT TYPE AND DATES COVERED Master's Thesis

4. TITLE AND SUBTITLE MODAL ANALYSIS OF THE PHALANX M61A1 CLOSE-IN WEAPONS SYSTEM

5. FUNDING NUMBERS

6. AUTHOR(S) Robert J. Hansberry, Capt. USMC

7. PERFORMING ORGANIZATION NAME(S) AND ADDRESS(ES)
Naval Postgraduate School
Monterey CA 93943-5000

8. PERFORMING ORGANIZATION REPORT NUMBER

9. SPONSORING/MONITORING AGENCY NAME(S) AND ADDRESS(ES)

10. SPONSORING/MONITORING AGENCY REPORT NUMBER

11. SUPPLEMENTARY NOTES The views expressed in this thesis are those of the author and do not reflect the official policy or position of the Department of Defense or the U.S. Government.

12a. DISTRIBUTION/AVAILABILITY STATEMENT
Approved for public release; distribution is unlimited.

12b. DISTRIBUTION CODE

13. ABSTRACT *(maximum 200 words)*A modal analysis of a PHALANX gun assembly was conducted in the laboratory at Naval Postgraduate School. The goal of this analysis is to provide a dynamical description of the gun for studies of the effects of gun modifications on bullet dispersion.

Accelerometer data were collected from five locations on the topmost barrel of the barrel assembly while the gun was being excited at the barrel tips with a swept sine forcing signal. This was done for five configurations of the gun, four of which did not include the production muzzle restraint, and the fifth that did. Frequency response data (vertical displacement/vertical force) were processed using the STARModal modal analysis software to extract modal parameters (frequencies, damping, and mode shapes) for frequencies up to 500Hz.

For the four unrestrained configurations, there were no major differences in frequency response spectra, modal frequencies, or modal shapes. Eight modes were identified below 500Hz. For some modes the shape of the barrel assembly motion was very similar, suggesting that other structural responses might be present.

The fifth configuration, with muzzle restraint, was distinct from the others in all categories, generally displaying lower modal frequencies and a higher modal frequency density. Thirteen modes were identified below 500Hz for this configuration. Again, there was some repetition of barrel assembly shapes for different modes.

This study shows that the addition of the muzzle restraint, which was designed to reduce barrel tip vibration has resulted in a much higher modal density for frequencies above about 125Hz. This is significant, since it is known that the frequency spectrum of the forcing function of a firing bullet has significant amplitude above 125Hz.

Recommendations are made for follow-on investigations.

14. SUBJECT TERMS Modal Analysis, PHALANX, Star.			15. NUMBER OF PAGES 114
			16. PRICE CODE
17. SECURITY CLASSIFICATION OF REPORT Unclassified	18. SECURITY CLASSIFICATION OF THIS PAGE Unclassified	19. SECURITY CLASSIFICATION OF ABSTRACT Unclassified	20. LIMITATION OF ABSTRACT UL

NSN 7540-01-280-5500 Standard Form 298 (Rev. 2-89)
Prescribed by ANSI Std. 239-18 298-102

Approved for public release; distribution is unlimited.

MODAL ANALYSIS OF THE PHALANX M61A1 CLOSE-IN WEAPONS SYSTEM

by

Robert J. Hansberry
Captain, United States Marine Corps
B.S., University of Nevada, Las Vegas, 1983

Submitted in partial fulfillment
of the requirements for the degree of

MASTER OF SCIENCE IN APPLIED PHYSICS

from the

NAVAL POSTGRADUATE SCHOOL
December 1994

Author: [redacted]
Robert J. Hansberry

Approved by: [redacted]
Steven R. Baker, Thesis Advisor

[redacted]
Robert M. Keolian, Second Reader

[redacted]
William B. Colson, Chairman
Department of Physics

Accession For
NTIS GRA&I ☑
DTIC TAB ☐
Unannounced ☐
Justification
By
Distribution/
Availability Codes
Dist | Avail and/or Special
A-1

ABSTRACT

A modal analysis of a PHALANX gun assembly was conducted in the laboratory at Naval Postgraduate School. The goal of this analysis is to provide a dynamical description of the gun for studies of the effects of gun modifications on bullet dispersion.

Accelerometer data were collected from five locations on the topmost barrel of the barrel assembly while the gun was being excited at the barrel tips with a swept sine forcing signal. This was done for five configurations of the gun, four of which did not include the production muzzle restraint, and the fifth that did. Frequency response data (vertical displacement/vertical force) were processed using the STARModal modal analysis software to extract modal parameters (frequencies, damping, and mode shapes) for frequencies up to 500Hz.

For the four unrestrained configurations, there were no major differences in frequency response spectra, modal frequencies, or modal shapes. Eight modes were identified below 500Hz. For some modes the shape of the barrel assembly motion was very similar, suggesting that other structural responses might be present.

The fifth configuration, with muzzle restraint, was distinct from the others in all categories, generally displaying lower modal frequencies and a higher modal frequency density. Thirteen modes were identified below 500Hz for this configuration. Again, there was some repetition of barrel assembly shapes for different modes.

This study shows that the addition of the muzzle restraint, which was designed to reduce barrel tip vibration has resulted in a much higher modal density for frequencies above about 125Hz. This is significant, since it is known that the frequency spectrum of the forcing function of a firing bullet has significant amplitude above 125Hz.

Recommendations are made for follow-on investigations.

TABLE OF CONTENTS

I. INTRODUCTION 1
A. MODAL ANALYSIS 1
B. APPLICATION TO PHALANX 2

II. DESCRIPTION OF EXPERIMENTS 5
A. PHALANX GUN TEST CONFIGURATIONS 5
B. SHAKER EXCITATION 7
C. ACCELEROMETER LOCATIONS 8
D. MEASUREMENTS 10

III. STARMODAL ANALYSIS SYSTEM 15
A. STARMODAL SOFTWARE 15
B. STARMODAL DATA PROCESSING 15

IV. RESULTS 19
A. INTRODUCTION TO RESULTS 19
B. RESONANCE PEAK IDENTIFICATION 19
C. MODAL FREQUENCIES EXTRACTED BY STARMODAL . . . 21
D. MODAL SHAPES FOR CONFIGURATIONS WITHOUT MUZZLE RESTRAINT 25
E. MODAL SHAPES FOR CONFIGURATION WITH MUZZLE RESTRAINT 27

V. CONCLUSIONS 31
A. SUMMARY 31
B. SUGGESTIONS FOR FOLLOW-ON INVESTIGATIONS . . . 32

APPENDIX A. STARMODAL TUTORIAL 35
A. STARMODAL INITIALIZATION 35
B. STRUCTURAL GEOMETRY 36
C. DISK TRANSLATION 41
D. FRF ANALYSIS 43

APPENDIX B. ANALYZER INPUT AND MEASUREMENT STATES . . . 47

APPENDIX C. FREQUENCY RESPONSE FUNCTIONS FOR ACCELEROMETER LOCATION 1 49

APPENDIX D. FREQUENCY RESPONSE FUNCTIONS FOR ACCELEROMETER LOCATION 2 53

APPENDIX E. FREQUENCY RESPONSE FUNCTIONS FOR ACCELEROMETER LOCATION 3 57

APPENDIX F. FREQUENCY RESPONSE FUNCTIONS FOR ACCELEROMETER LOCATION 4 61

APPENDIX G. FREQUENCY RESPONSE FUNCTIONS FOR ACCELEROMETER LOCATION 5 65

APPENDIX H. MODAL SHAPES FOR CONFIGURATION 1 69

APPENDIX I. MODAL SHAPES FOR CONFIGURATION 2 73

APPENDIX J. MODAL SHAPES FOR CONFIGURATION 3 77

APPENDIX K. MODAL SHAPES FOR CONFIGURATION 4 81

APPENDIX L. MODAL SHAPES FOR CONFIGURATION 5 85

APPENDIX M. PCB 353B44 ACCELEROMETER CALIBRATION 89

APPENDIX N. BRÜEL AND KJÆR TYPE 8001 IMPEDANCE HEAD CALIBRATION 91

LIST OF REFERENCES 93

INITIAL DISTRIBUTION LIST 95

LIST OF FIGURES

Figure 1-1. PHALANX gun system. [from NAVSEA OP 4154 Vol. 1] 1
Figure 1-2. PHALANX Weapon Group. 2
Figure 2-1. PHALANX major components. 5
Figure 2-2. PHALANX laboratory set-up, without muzzle restraint. 6
Figure 2-3. Load inducing set-up. 6
Figure 2-4. Stinger arrangement at barrel tips. 8
Figure 2-5. PHALANX with uppermost barrel at 12 o'clock. 9
Figure 2-6. PHALANX with uppermost barrel offset to firing position. 10
Figure 2-7. Example of acceleration FRF (top) and corresponding displacement FRF (bottom). 12
Figure 2-8. Displacement FRF's measured by H-P analyzer at each of the five points for configuration 5. . 14
Figure 4-1. Driving point (point 5) displacement FRF's for configurations 1 through 5. 20
Figure 4-2. Modal frequencies for each configuration. . 23
Figure 4-3. Mode 1, Config 1. 25
Figure 4-4. Mode 2, Config 1. 25
Figure 4-5. Mode 3, Config 1. 25
Figure 4-6. Mode 4, Config 1. 25
Figure 4-7. Mode 5, Config 1. 26
Figure 4-8. Mode 6, Config 1. 26
Figure 4-9. Mode 7, Config 1. 26
Figure 4-10. Mode 8, Config 1. 26
Figure 4-11. Mode 9, Config 1. 26
Figure 4-12. Mode 1, Config 5. 28
Figure 4-13. Mode 2, Config 5. 28
Figure 4-14. Mode 3, Config 5. 28

Figure 4-15. Mode 4, Config 5. 28
Figure 4-16. Mode 5, Config 5. 28
Figure 4-17. Mode 6, Config 5. 28
Figure 4-18. Mode 7, Config 5. 28
Figure 4-19. Mode 8, Config 5. 28
Figure 4-20. Mode 9, Config 5. 29
Figure 4-21. Mode 10, Config 5. 29
Figure 4-22. Mode 11, Config 5. 29
Figure 4-23. Mode 12, Config 5. 29
Figure 4-24. Mode 13, Config 5. 29
Figure A-1. Structural geometry and coordinate system used for PHALANX modal identification. 36
Figure B-1. Measurement state for H-P analyzer during data collection. 48
Figure B-2. Input state for H-P analyzer during data collection. 48
Figure C-1. FRF's recorded at accelerometer location 1 . 50
Figure D-1. FRF's recorded at accelerometer location 2 . 54
Figure E-1. FRF's recorded at accelerometer location 3 . 58
Figure F-1. FRF's recorded at accelerometer location 4 . 62
Figure G-1. FRF's recorded at accelerometer location 5 . 66
Figure I-1. Mode 1, Config 2. 74
Figure I-2. Mode 2, Config 2. 74
Figure I-3. Mode 3, Config 2. 74
Figure I-4. Mode 4, Config 2. 74
Figure I-5. Mode 5, Config 2. 74
Figure I-6. Mode 6, Config 2. 74
Figure I-7. Mode 7, Config 2. 74
Figure J-1. Mode 1, Config 3. 78
Figure J-2. Mode 2, Config 3. 78
Figure J-3. Mode 3, Config 3. 78
Figure J-4. Mode 4, Config 3. 78
Figure J-5. Mode 5, Config 3. 78
Figure J-6. Mode 6, Config 3. 78

Figure J-7. Mode 7, Config 3. 78
Figure J-8. Mode 8, Config 3. 78
Figure K-1. Mode 1, Config 4. 82
Figure K-2. Mode 2, Config 4. 82
Figure K-3. Mode 3, Config 4. 82
Figure K-4. Mode 4, Config 4. 82
Figure K-5. Mode 5, Config 4. 82
Figure K-6. Mode 6, Config 4. 82
Figure K-7. Mode 7, Config 4. 82
Figure K-8. Mode 8, Config 4. 82

LIST OF TABLES

Table 3-1. Major Steps of Parameter Identification in STAR. 18
Table 4-1. Table of modal frequencies and %damping for each configuration. 21
Table A-1. Coordinates Table example for PHALANX. . . . 38
Table A-2. Display Sequence table example for PHALANX. . 39
Table C-1. Resonance peak frequencies for accelerometer location 1. 51
Table D-1. Resonance peak frequencies for accelerometer location 2. 55
Table E-1. Resonance peak frequencies for accelerometer location 3. 59
Table F-1. Resonance peak frequencies for accelerometer location 4. 63
Table G-1. Resonance peak frequencies for accelerometer location 5. 67
Table H-1. Amplitudes and phases computed by STARModal for configuration 1. 70
Table I-1. Amplitudes and phases computed by STARModal for configuration 2. 75
Table J-1. Amplitudes and phases computed by STARModal for configuration 3. 79
Table K-1. Amplitudes and phases computed by STARModal for configuration 4. 83
Table L-1. Amplitudes and phases computed by STARModal for configuration 5. 86

ACKNOWLEDGEMENT

The author would like to express his gratitude to Yuji Wilson and the PHALANX working group at both Port Hueneme, Naval Surface Warfare Center and China Lake, Naval Weapons facility for their support and inspiration. Thanks also to Mike Hatch for sharing his time to lend guidance and an engineer's point of view. Thanks as well to Drs. Steven R. Baker and Robert M. Keolian for their professional insight and long, arduous hours spent preparing this final product. In addition, a special thanks to David Cela, partner extraordinaire, for his diligence and enthusiasm.

Finally, the author would like to thank his family, especially his wife, Lorraine, and daughter, Margaux, for their patience and understanding during this particularly trying endeavor. They have been with him from the beginning. And, no expression of appreciation would be complete without acknowledging the predominant force his mother, Machiko, has been, continually emphasizing the importance of education and aspiration.

I. INTRODUCTION

A. MODAL ANALYSIS

Vibration is the result of dynamic forces acting upon a structure. Effects of vibration range from wear and reduced performance to mechanical failure.

Most vibration problems can be linked to resonance phenomena. Resonance is a vibrational state that occurs when dynamic forces on a structure excite natural modes of vibration. The increased vibrational intensity that accompanies resonance can lead to the aforementioned negative effects. A study of the modes of a structure not only provides the frequencies for which potential problems might arise, but also forms the basis for the complete dynamic description of the structure. This description can be used to validate a mathematical model of the structure. In the investigation described in this thesis, modal analysis was applied to a PHALANX six-barrel, 20mm, automatic gun.

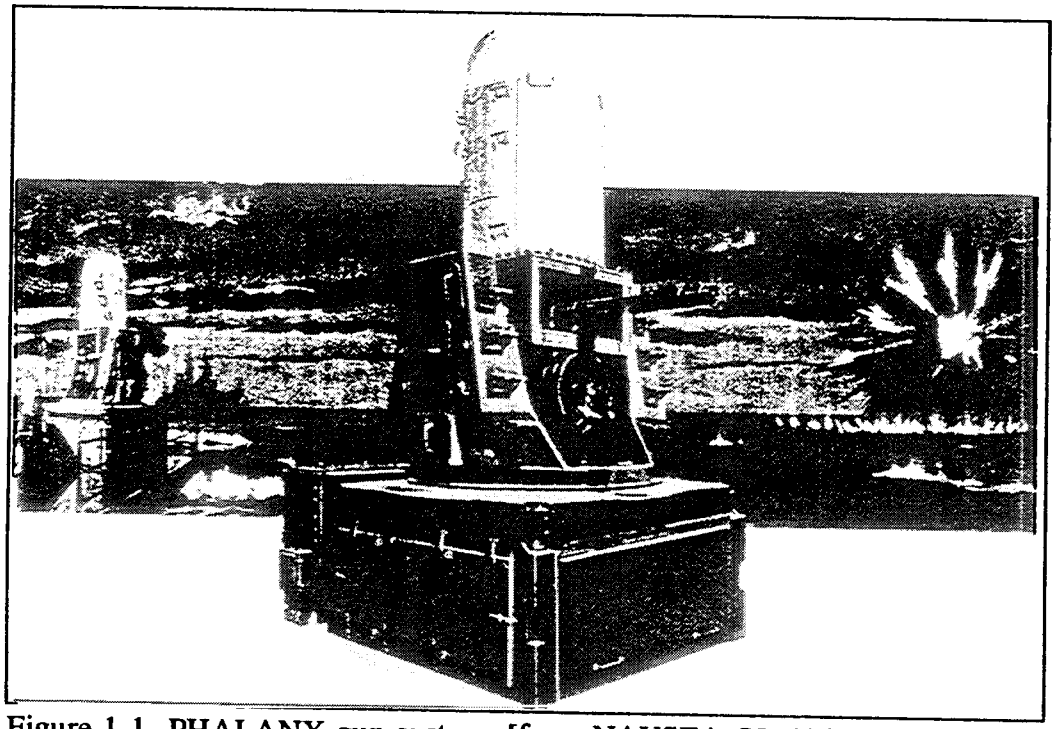

Figure 1-1. PHALANX gun system. [from NAVSEA OP 4154 Vol. 1]

B. APPLICATION TO PHALANX

The PHALANX 20mm M61A1 Close-in Weapons System (CIWS) (Figure 1-1) is the U.S. Navy's final defense against anti-ship missiles. PHALANX is a six-barrel, hydraulic- or electrically-driven, rotary-action, 20mm automatic gun. It is approximately 1.8m (72 in.) long and 114kg (252 lbs.) in weight. The PHALANX Weapon Group (Figure 1-2) that houses the gun reveals several sub-groups that contain mechanisms which contribute dynamic loads to the structure. The gun's structural response to these loads can be predicted using the results of modal analysis, i.e. modal frequencies and shapes. [Refs 1 and 2]

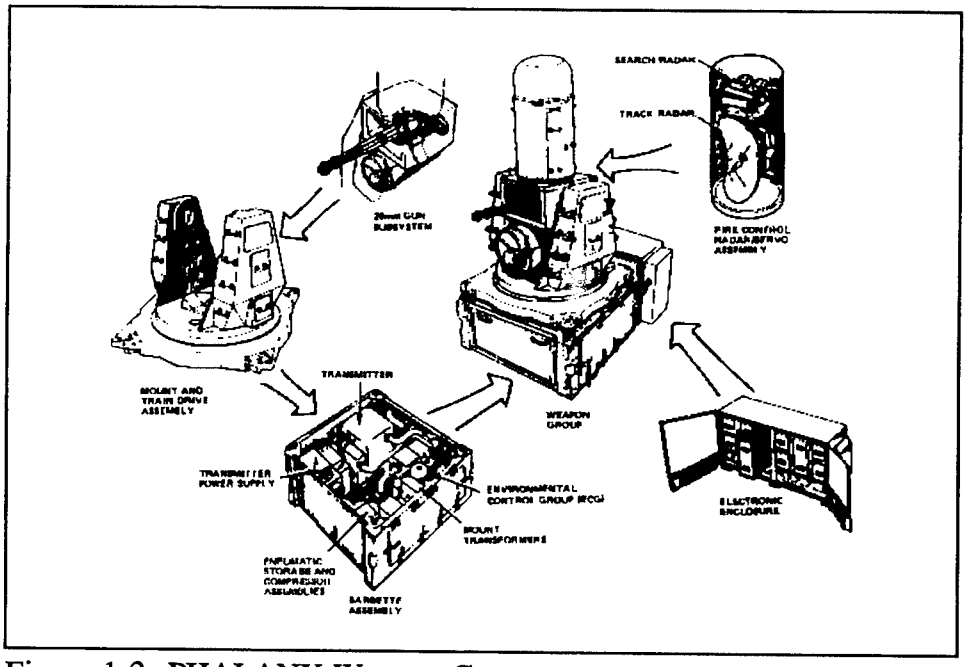

Figure 1-2. PHALANX Weapon Group.

Recently, there has been increased emphasis placed on improving the intercept capability of PHALANX. Current models

experience so much ballistic dispersion (a statistical description of bullets off target) that there can be no guarantee of target destruction without significant damage from secondary impacts of target fragments when engaging faster, more technologically advanced missiles. This dispersion is partially related to barrel tip motion that is aggravated by the excitation of barrel assembly modes of vibration. The complexity of the gun system makes the identification of the source(s) of this excitation difficult, but not impossible.

The goal of this study is to develop a method of measuring the frequency response of a fully deployed PHALANX system in order to describe its natural modes of vibration. The results will be used to validate the finite element model (FEM) which has been developed to describe the gun. [Refs 3 and 4] This will yield a test-validated model with which one can economically examine the effects of modifications on dispersion.

II. DESCRIPTION OF EXPERIMENTS

A. PHALANX GUN TEST CONFIGURATIONS

Frequency response measurements were conducted on an actual PHALANX gun in the laboratory. Due to size limitations, the entire PHALANX shipboard module (depicted in Figure 1-2) could not be accommodated in the laboratory.

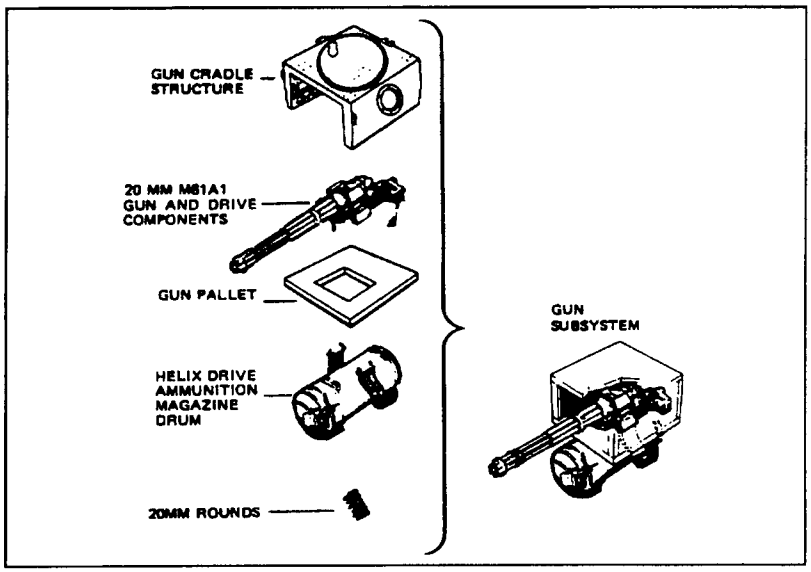

Figure 2-1. PHALANX major components.

Instead, the gun (without drive components or ammunition feed guides), gun cradle structure, and gun pallet (see Figure 2-1) were assembled and set on three cork and rubber dampers on the laboratory floor, located on the foundation in the basement of the Naval Postgraduate School's Spanagel Hall (see Figure 2-2). Two of the dampers were placed under the forward part of the gun pallet just inside the clevises that anchor the legs of the muzzle restraint. The third was centered at the rear of the gun pallet. These dampers were placed so that there was no rocking of the gun pallet about any axis.

Five configurations of this assembly were tested. These were distinguished by the position of the topmost barrel,

whether the barrel assembly was free or under an axial load similar to that experienced when a bullet is fired, and whether or not the muzzle restraint was attached.

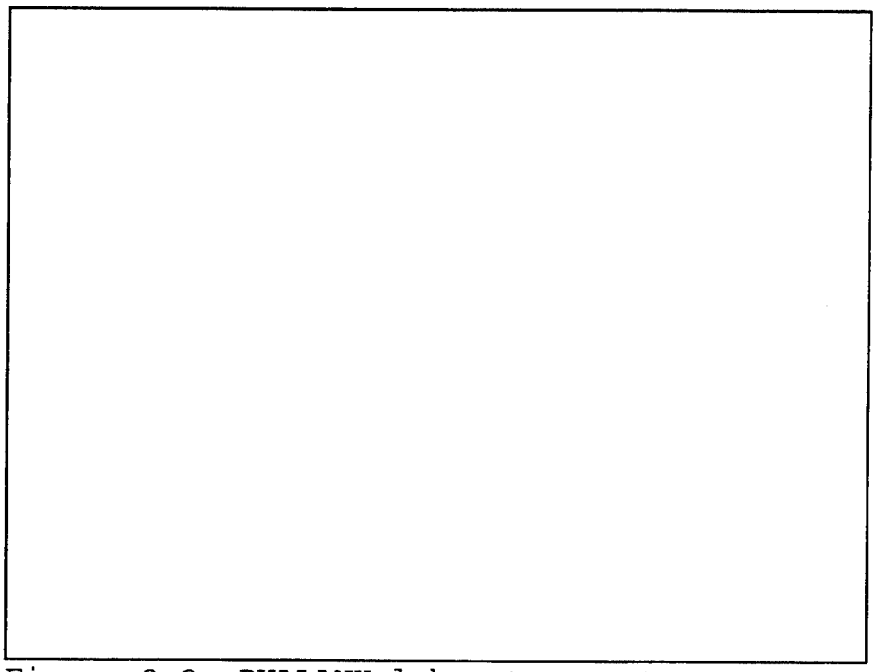

Figure 2-2. PHALANX laboratory set-up, without muzzle restraint.

The load on the gun was supplied by an aluminum ball large enough to lodge in the forward hole in the center of the stub rotor (see Figure 2-3). The ball was pulled back by an eyebolt screwed through the center of the ball.

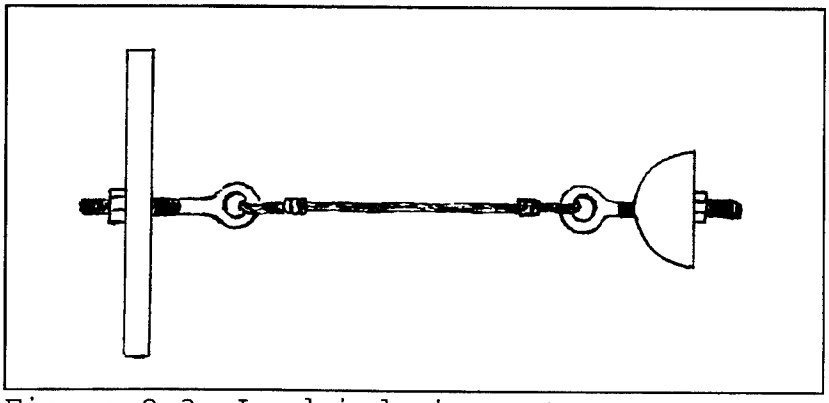

Figure 2-3. Load inducing set-up.

A high tensile strength cable attached to the eyebolt was threaded through the center of the gun and connected to another eyebolt bolted through a crossbar braced across the back end of the gun cradle structure. Care was taken to ensure that the only contact with the gun itself was where the ball pulled back on the stub rotor. It was necessary to temporarily remove one of the barrels to fit the ball into the stub rotor hole.

The tested configurations were:

1. topmost barrel at 12 o'clock position (top dead center), no load, and no muzzle restraint,
2. topmost barrel at 12 o'clock, loaded, and no muzzle restraint,
3. topmost barrel at firing position, no load, and no muzzle restraint,
4. topmost barrel at firing position, loaded, and no muzzle restraint, and,
5. topmost barrel at firing position, loaded, and muzzle restraint attached.

B. SHAKER EXCITATION

Dynamic force was applied to the muzzle end of the gun using an Acoustics Power Source Perma-Dyne model 120S [Ref 5] shaker and amplifier system placed directly on the lab floor (see Figure 2-4). A stinger assembly consisting of a 215mm long, 10-32 threaded rod, locking nuts, and a Brüel and Kjær model 8001 impedance head [Ref 6] was mounted on the shaker. The impedance head, used to measure the force to the driving point, was attached to a rectangular, aluminum plate (7mm x 48mm x 53mm) in a standard drive configuration. In the center of the plate, at the approximate height of the gun axis, was a hole that was fitted over an expanding aluminum cylinder that was inserted into the locking lug, which secures the muzzle clamp onto the end of the barrels.

Excitation applied to the amplifier input consisted of swept sinusoidal signal of 2mVRMS stepped from 2-500Hz in 1.245Hz increments (498Hz span divided by the 401 points per sweep, as set on the analyzer, equals 1.245Hz per point). The signal source was a Hewlett-Packard 35665A 2-channel signal analyzer [Ref 7]. Amplification was supplied by an Acoustics Power Systems model 114 power amplifier [Ref 5], which has a fixed gain, operated in voltage mode. The lower frequency limit of 2Hz was chosen as there were no resonant peaks visible below this frequency. Removing the 0-2Hz portion of the sweep reduced the measurement time significantly. The upper frequency limit was arbitrarily set to give enough resonant peaks to derive an adequate set of modes to compare with FEM derived modes. The measurement and input states of the analyzer are given in Appendix B.

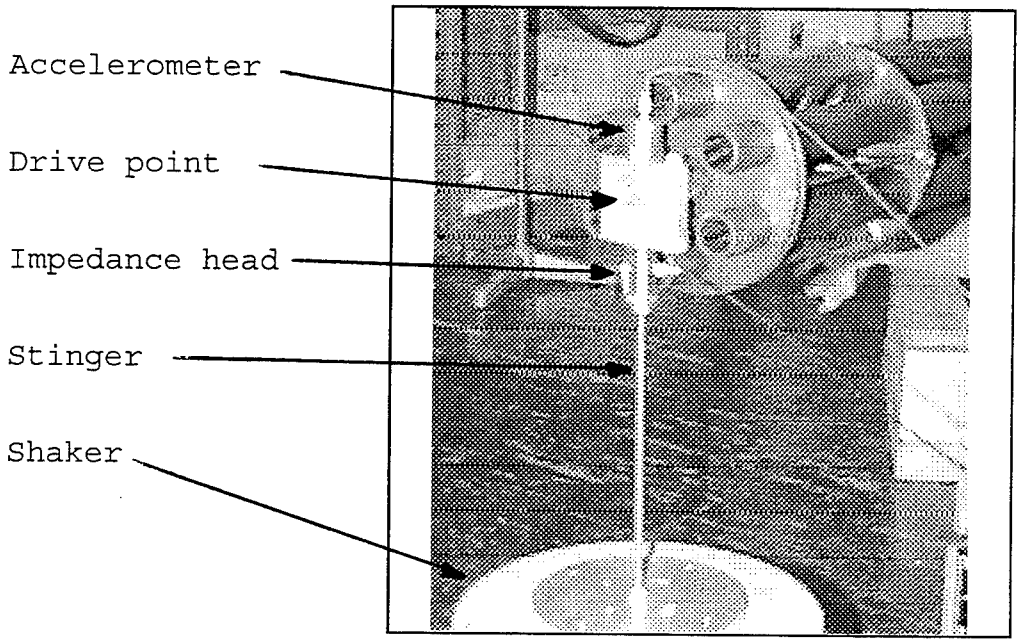

Figure 2-4. Stinger arrangement at barrel tips.

C. ACCELEROMETER LOCATIONS

The acceleration response to the force applied by the shaker was measured with a PCB model 353B44 accelerometer [Ref 8]. The accelerometer was mounted to studs which had been

cemented with epoxy to selected gun locations. The response signal was amplified using a PCB model 482A17 preamplifier [Ref 8]. The calibration sheet for the accelerometer is given in Appendix M.

Five accelerometer locations along the barrel assembly were chosen for their potential to yield the best description of modal characteristics with the least number of accelerometer attachments. Figure 2-5 shows the accelerometer mount locations (barely visible as light spots on the barrel) on the topmost barrel used for configurations 1 and 2, when it is at twelve o'clock relative to the barrel assembly longitudinal axis. Note the collinearity of the mount locations.

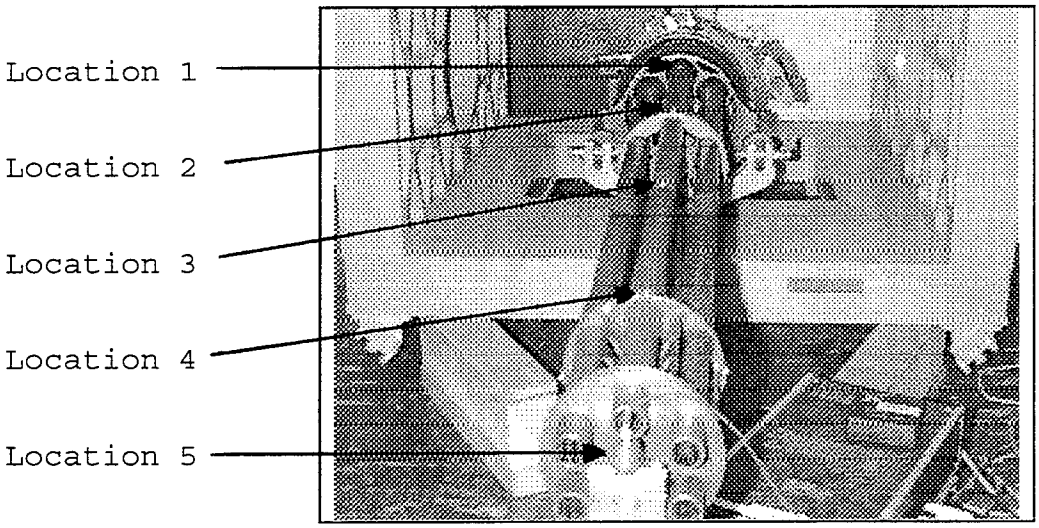

Figure 2-5. PHALANX with uppermost barrel at 12 o'clock.

The first accelerometer location is at the base of the topmost barrel, as close as possible to where the barrel inserts into the stub rotor. The second location is on top of

the mid-barrel clamp. The third location is at the center of the topmost barrel, between the mid-barrel and muzzle clamps. The fourth location is on top of the back ring of the muzzle clamp. The fifth location is on top of the aluminum plate that attached the impedance head to the front of the muzzle clamp (see Figure 2-4).

Accelerometer locations for measurements taken when the topmost barrel was in the firing position (~11° before TDC) are shown in Figure 2-6. These locations were used for configurations 3, 4, and 5. Their locations in the z-direction (down the barrel) are identical to those of the TDC configuration. However, they are not collinear; the two locations on the topmost barrel, points 1 and 3, are laterally displaced from the barrel assembly axis (see Figure 2-6).

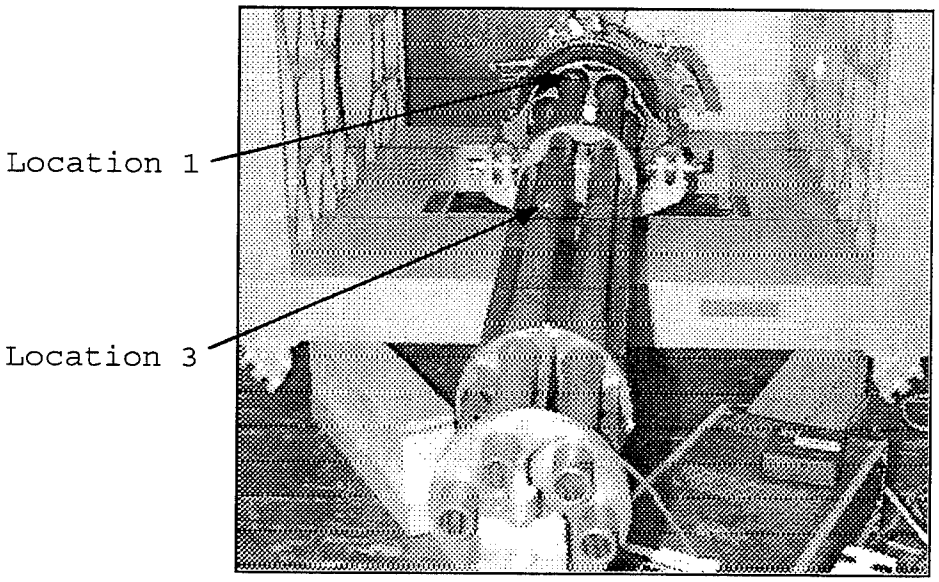

Figure 2-6. PHALANX with uppermost barrel offset to firing position.

D. MEASUREMENTS

The force voltage signal from the impedance head and the voltage signal from the accelerometer were input to the Hewlett-Packard analyzer, which combined the two in the

frequency domain to obtain the frequency response, described below. For all measurements the force was applied at a fixed position, the barrel tips, while the acceleration was measured at various positions on the gun assembly.

The frequency response function, or FRF, represents the complex ratio of output to input as a function of frequency. Mathematically, it can be defined as:

$$H(\omega) = \frac{\alpha(\omega)}{F(\omega)}, \qquad (2\text{-}1)$$

where $H(\omega)$ is the FRF, $\alpha(\omega)$ is acceleration, and $F(\omega)$ is the applied force. The physical interpretation of this equation is that the FRF is the modification of an input force, F, for a particular frequency, ω, that results in an acceleration, α. This modification is the multiplication of the amplitudes of F ($|F|$) and H ($|H|$), while the phase between output and input is shifted by the phase introduced by H. [Ref 9]

For the PHALANX system, the displacement of the barrels is more informative than the acceleration, particularly when studying bullet dispersion. In order to transform the acceleration FRF to one of displacement requires a review of the equations of motion and some Fourier manipulation. The displacement, $x(t)$, and acceleration, $a(t)$, are related to their Fourier transforms, $X(\omega)$ and $\alpha(\omega)$, respectively, by:

$$x(t) = \int \chi(\omega)\, e^{(j\omega t)}\, d\omega \qquad (2\text{-}2)$$

and,

$$a(t) = \int \alpha(\omega)\, e^{j\omega t} d\omega . \qquad (2\text{-}3)$$

But,

$$a(t) = \frac{d^2}{dt^2} x(t) = \int \chi(\omega)\, (j\omega)^2 e^{j\omega t} d\omega, \qquad (2\text{-}4)$$

so, equating integrands,

$$\chi(\omega) = \alpha(\omega) \frac{1}{(j\omega)^2}. \qquad (2\text{-}5)$$

[Ref 10]

The H-P analyzer can be set to divide the measured acceleration frequency response by $(j\omega)^2$, thereby producing the displacement FRF. Figure 2-7 presents an example of an acceleration FRF and its corresponding displacement FRF. Note how the differences between the magnitude of the fundamental mode at around 19Hz and subsequent modes are more pronounced in the displacement FRF, thereby isolating modes that contribute more significantly to displacement. Displacement FRF's were recorded for the five gun configurations at the five accelerometer positions on the topmost barrel.

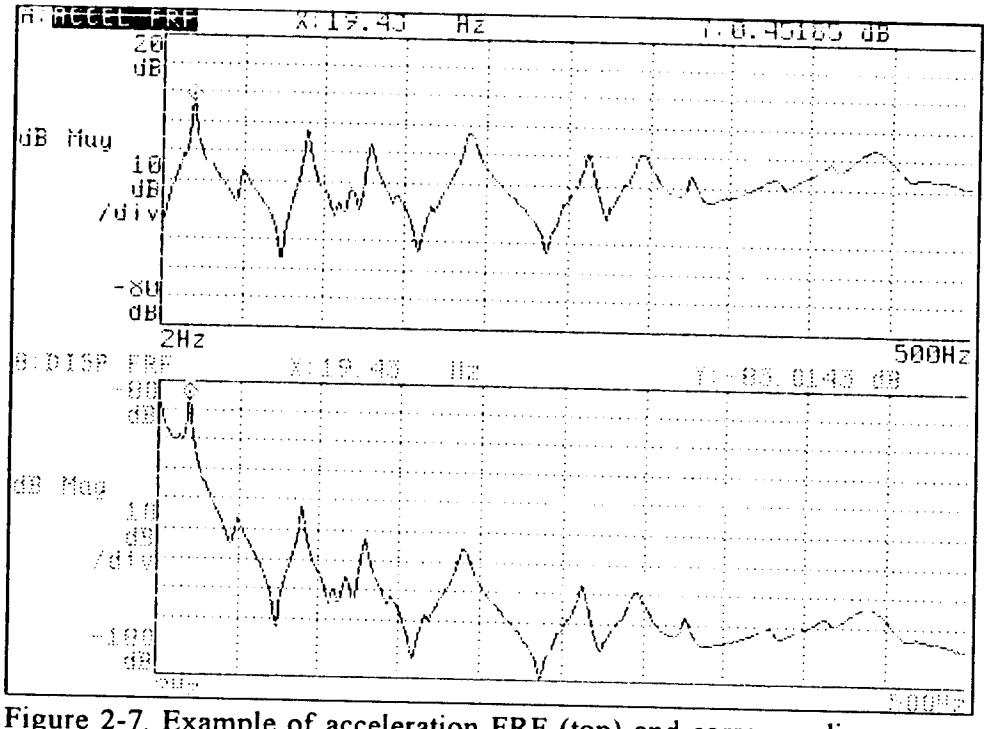

Figure 2-7. Example of acceleration FRF (top) and corresponding displacement FRF (bottom).

Figure 2-8, on the following page, is a sample of the displacement FRF's measured by the H-P analyzer. The sample is from measurements taken at each of the five points for configuration 5. Displacement FRF's taken at each of the five points for all configurations can be found in Appendices C through G.

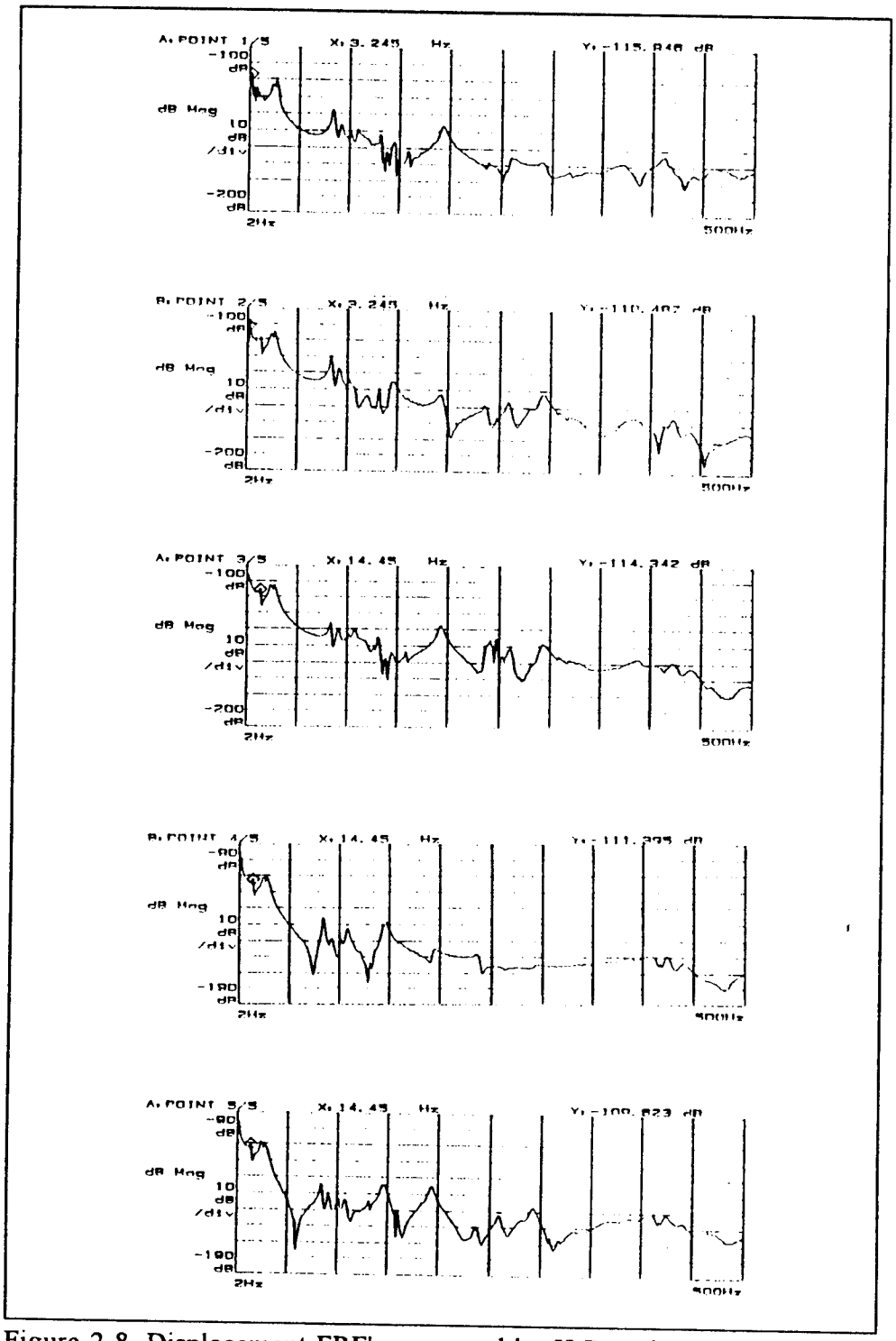

Figure 2-8. Displacement FRF's measured by H-P analyzer at each of the five points for configuration 5.

III. STARMODAL ANALYSIS SYSTEM

A. STARMODAL SOFTWARE

The frequency response spectra taken at the five accelerometer locations for each configuration were translated into files that could be read by the Structural Measurement Systems (SMS) Structural Testing, Analysis, and Reporting (STAR) System [Ref 11] software using STAR's Disk Translator.

STARModal is one in a series of STAR System software products for testing and analyzing the dynamics of mechanical structures. It uses the FRF method to identify modal parameters and display the modes in animation. The FRF can either be imported directly via GPIB (IEEE488) interface bus or from disk storage.

The complete STARModal procedure from input of disk storage data to animation of structure modes is given in Appendix A.

B. STARMODAL DATA PROCESSING

Using the FRF method, STARModal identifies the modal parameters of a structure. Frequency response functions made with the H-P signal analyzer are first stored on disk, then translated into STAR compatible files by the Disk Translator for processing (see Appendix A). During processing, an analytical model of the FRF is fit (in a least-squares sense) to the measured data and, as a result, the modal parameters are identified. This is the curve fitting process. [Ref 12]

The procedure to identify modal parameters has several major steps. They are outlined in Table 3-1. [Ref 12]

The first step in the modal parameter identification process is the determination of how many modes are present in the frequency range of the data. Each mode is represented by a peak in the data, called a resonance peak. There should be

a modal peak at approximately the same frequency in the FRF for every measurement location. If a measurement point is at or near a node of a certain mode, where the mode shape is zero, the FRF will not show (much of) a peak for that mode. If a peak at a particular frequency is negligible or absent for a significant fraction of FRF's, modal parameters will not be identified by STARModal for that peak and there will not be a one-to-one correspondence between resonance peaks and modes. A local mode is one for which a modal peak does not appear in a large number of measurements, i.e. a mode with zero shape for many measurement locations. [Ref 12]

Table 3-1. Major Steps of Parameter Identification in STAR.

1. Identify the number of modes in the measurements both visually and with STAR's Modal Peaks function.
2. Set up curve fitting bands; this entails bracketing a frequency band for one or more modes, setting a mode number range, and selecting a curve fitting method.
3. Use the Autofit feature in STAR to perform a simultaneous curve fit to data in the selected bands for all FRF's.
4. Examine results using STAR's animation feature.

Next is the bracketing of curve fitting bands, each band representing the width, or frequency range, of a resonance peak. The hand-selected data for all measurement locations

will be simultaneously curve fit to analytic expressions for the FRF's using one of the methods offered by STARModal.

In the third step the user executes the STARModal autofit feature which performs the curve fitting. The data are fit to a polynomial function using the Rational Fraction Least Squares (RFLS) method. The modal frequencies, mode shapes, and the percent of critical damping (the modal parameters) for each mode are calculated. These values are stored in a table to be used in the animation display.

Examination of the results entails nothing more than clicking on the **Show Structure** command in the **Gateway** menu. The structure is automatically presented in the animation window, waving in its first mode.

A complete description of the use of STARModal to accomplish parameter identification is provided in Appendix A.

IV. RESULTS

A. INTRODUCTION TO RESULTS

Three types of results are discussed in this chapter. First, are the frequency response functions that were produced by the H-P analyzer. The complete record of FRF's for the five accelerometer locations for all configurations can be found, arranged by point of measurement, in Appendices C through G. Each appendix has the FRF analyzer traces recorded for each configuration and a table that lists the resonance peak frequencies visually identified on those traces. The importance of these traces is that they were the data sources used to identify the resonance peaks from which the curve fit bands were selected. A measurement set of five FRF's, representing data taken from each accelerometer location for one configuration, was set up in a file in STARModal. Each was brought up on the STARModal **Measurement** window to identify the trace with the greatest number of well-defined peaks. Curve fitting bands were selected from this trace, and STARModal used them to extract modal parameters.

The second and third results discussed are the modal frequencies and the mode shapes extracted by STARModal, respectively. The process by which these were obtained was discussed in Chapter III, Section B.

B. RESONANCE PEAK IDENTIFICATION

The frequency response functions recorded by the analyzer were very similar for the four gun configurations which did not include the muzzle restraint (see Figure 4-1). All discrepancies were small compared to the level of the prominent peaks. The similarity between these traces shows that the dependence of the modal response of the gun on barrel position and static load is small. That is why data for the

muzzle restraint configuration were recorded for one configuration only.

Frequencies for the resonance peaks observed below 500Hz for the first four configurations range from 19Hz to around 450Hz. The number of peaks found varies from 6 to 12. For the most part, at lower frequencies, the resonant peaks for one configuration coincide with those for any of the other three.

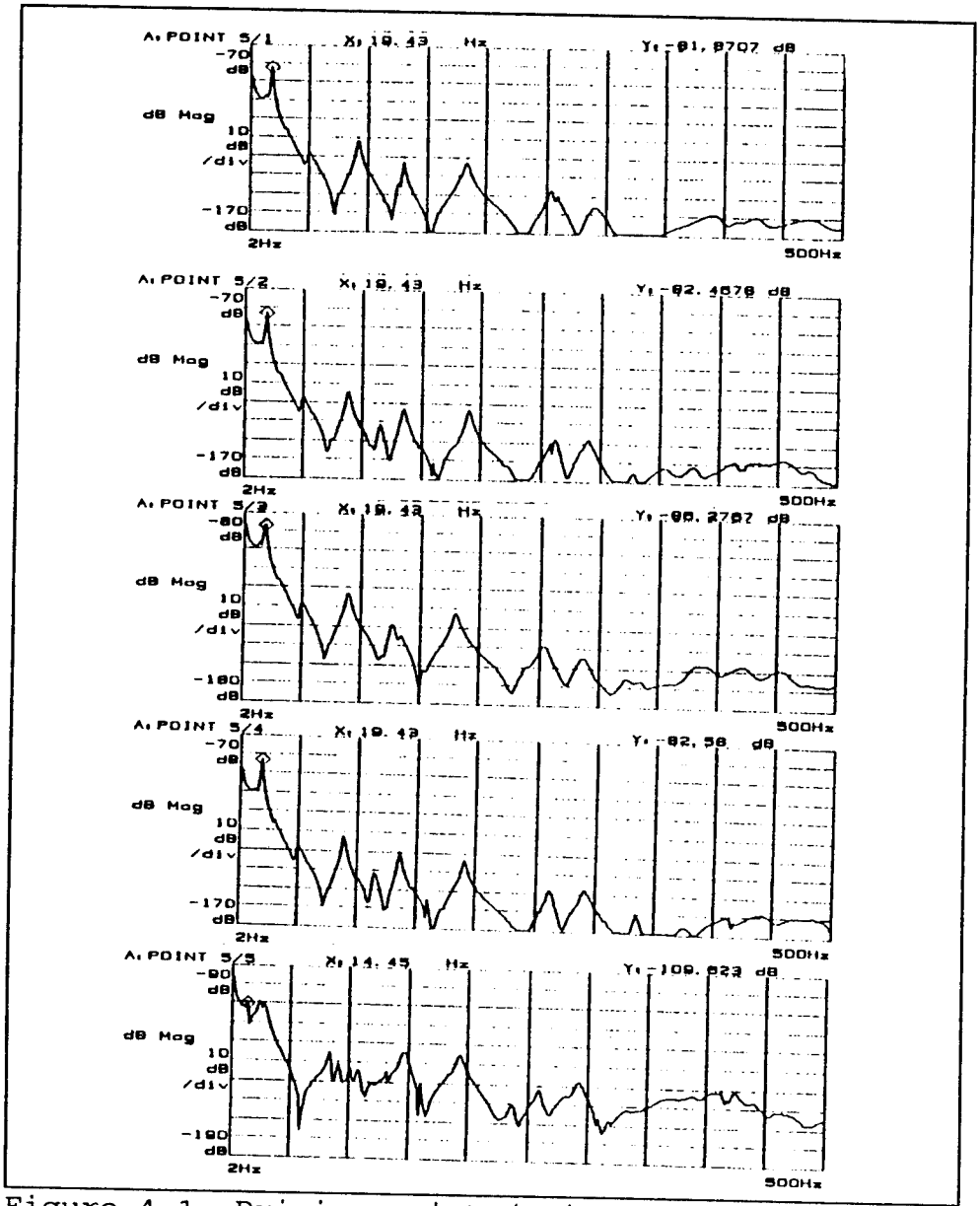

Figure 4-1. Driving point (point 5) displacement FRF's for configurations 1 through 5.

While the first four configurations had very similarFRF's, the FRF for the fifth configuration was markedly different (see Figure 4-1). In general, the resonance peaks for configuration 5 occurred over a wider range of frequencies and in greater number. There were 9 to 16 resonance peaks observed below 500Hz, ranging from approximately 3 to 440Hz.

The shape of the peaks was also different for the fifth configuration. The four unrestrained configurations had sharp, relatively isolated, well-defined peaks in their FRF's. The restrained configuration showed jagged, and relatively strong, peaks, most notably in the low, 24-28Hz frequency region.

C. MODAL FREQUENCIES EXTRACTED BY STARMODAL

Table 4-1 summarizes the modal frequencies and percent of critical damping that STARModal extracted from data taken from the five measurement locations for each configuration. The corresponding mode shapes can be found in Appendices H through L. No more than nine modal frequencies were identified by the STARModal process for the four configurations that did not include the muzzle restraint. The average fundamental frequency is 19.08±0.13Hz for these four configurations.

MODE	CONFIG 1		CONFIG 2		CONFIG 3		CONFIG 4		CONFIG 5	
	Freq	%Dmp	Freq	%Dmp	Freq	%Dmp	Freq	%Dmp	Freq	%Dmp
1	19.16	2.56	19.16	3.33	18.88	3.14	19.1	3.85	24.71	1.67
2	51.54	1.47	89.4	1.08	51.51	2.21	51.7	3.5	84.51	0.88
3	92.48	1.12	115.38	1.26	90.11	2.55	89.6	1.02	101.37	0.99
4	130.65	0.60	135.21	1.00	127.75	1.06	115.43	1.28	120.23	2.23
5	183.98	1.19	190.5	0.77	180.4	1.22	136.37	0.84	132.23	0.43
6	256.49	0.90	263.82	0.45	253.79	0.73	191.14	0.87	145.84	1.44
7	392.82	2.10	291.91	0.96	392.38	3.66	262.82	0.75	194.02	1.15
8	428.57	1.21			420.11	2.58	291.42	1.09	238.41	1.1
9									260.28	0.82
10									293.93	1.32
11									383.35	2.31
12									423.17	0.46
13									492.86	1.21

Table 4-1. Table of modal frequencies and %damping for each configuration.

As a quick check to see if this value is respectable, the fundamental frequency was calculated for a simpler, yet similar structure. The structure chosen was a tubular bar clamped at one end to simulate the cylindrical gun structure anchored in the stub rotor. The fundamental frequency can be calculated from the following equation:

$$f_0 = \frac{0.5598}{L^2}\sqrt{\frac{Y R^2}{\rho}}, \qquad (4\text{-}1)$$

where L is the length of the bar, Y is Young's modulus, R the radius of gyration, and ρ the density. [Ref 13] For the gun, the applicable values are:

$$L = 1.31\text{m} = 131\text{cm},$$

$$Y = 19\text{x}10^{10}\text{Pa} = 19\text{x}10^{11}\text{dynes/cm}^2\text{(steel)},$$

and, $\rho = 7700\text{kg/m}^3 = 7.7\text{g/cm}^3$(again, for steel).

The radius of gyration for a cylinder is:

$$R = \frac{\sqrt{a^2+b^2}}{2},$$

where a is the inner radius of the cylinder and b is the outer radius. Using 3.0cm as the inner radius and 6.5cm as the outer, measured at the muzzle clamp, gives a radius of gyration of 3.58cm for the gun. Plugging these values into equation 4-1 gives a frequency of 57.88Hz, which, though almost three times larger than the 19.43Hz given by the FRF's, is of the same magnitude. A tubular bar made of the same material as PHALANX has a larger radius of gyration than the six-barrels of the gun system and would be expected to have a higher fundamental frequency.

If, the parameters for just one barrel were used, instead of using parameters for the whole barrel assembly, the only change in the equation above would be the radius of gyration. For one barrel, a is approximately 1cm, and b averages 1.6cm

for the tapered barrels. This gives a radius of gyration of about 0.94cm. Using this in equation 4-1 leads to a frequency of about 15.2Hz, a much closer value to the 18-19Hz measured. This suggests that the barrel clamps are not very effective in restraining relative motion between the barrels.

Figure 4-2 is a graphic representation of the modal frequency progression for each configuration.

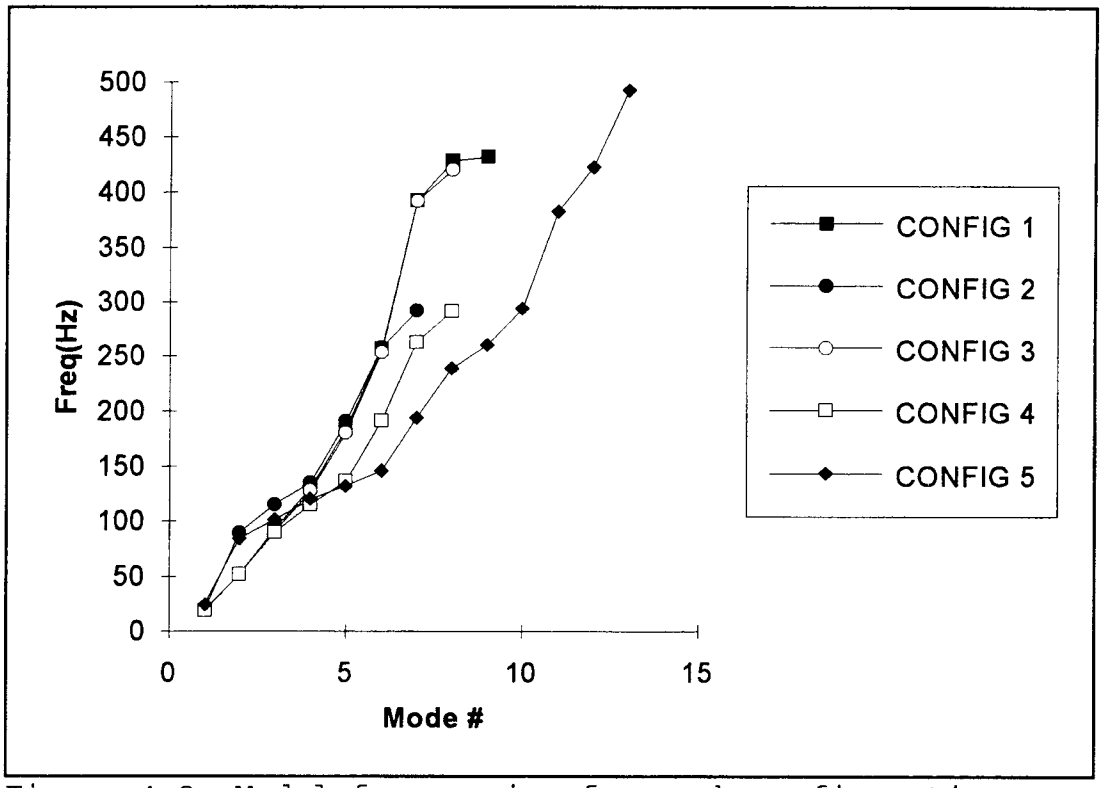

Figure 4-2. Modal frequencies for each configuration.

Looking at the modal frequency curves for the first four configurations, there are some places where the values match and others where deviations are evident. The two configurations for which no axial load was applied (i.e. 1 and 3) lie pretty much atop one another (they are obscured by the curve for configuration 4 below 125Hz). Except for the one mode that is lacking for configuration 2 at about 50Hz, the graphs of configurations 2 and 4 also coincide with

configurations 1 and 3 up to 250Hz, or so. There is no apparent reason that STARModal did not find a mode at 50Hz for configuration 2; the FRF's for all accelerometer locations but location 2 show a peak at about 50Hz. Reprocessing of the data gave the same results.

Another obvious discrepancy occurs at about 290Hz, with configurations 2 and 4 showing an "extra" mode. The discrepancy in the modal frequency spectra near 290Hz for configurations 1 to 4 is perhaps understandable from the FRF's. Recall that STARModal will not acknowledge a mode if the modal peaks are absent in a large number of measurements (see Chap. III, Section B). Looking at the resonant peak frequencies for configurations 1 to 4 in the appendices, both 2 and 4 have peaks that correspond to 290Hz for four out five points. Configurations 1 and 3, on the other hand, correspond for only three out of the five. If the cutoff for modal recognition is between 3/5 and 4/5, identification of a mode for configurations 1 and 3 would be suppressed.

Dismissing the discrepancies between the modal frequency spectra for the first four configurations as minor, the conclusion is reached that the modal structure for these four configurations is virtually the same.

Alterations to any structure can be expected to change its modal response. Such is the case for configuration 5, for which the muzzle restraint was attached. Up to around 125Hz, the modal frequencies coincide with those of the other four configurations. Beyond this, the density of modes for configuration 5 increases dramatically. There are, at most, five modes between 125Hz and 500Hz for configurations 1 through 4; there are nine for configuration 5. This is an undesirable feature, since it makes it more likely that a mode will be excited by the forces exerted when the gun is fired.

D. MODAL SHAPES FOR CONFIGURATIONS WITHOUT MUZZLE RESTRAINT

Modal shapes derived by STARModal (and a table of amplitudes and phase angles) are included in Appendices H through L. They are arranged by configuration in numerical order. Like the resonance peaks, the shapes identified for the four unrestrained configurations are very similar, particularly at lower frequencies.

Since the modal shapes for these configurations are similar, one was chosen as an example. Figures 4-3 through 4-11 show the mode shapes and frequencies for configuration 1, one for which the most modes were identified (nine). Although it is tempting to interpret the mode shapes by comparison to a fixed-free cantilevered bar, the correspondence is weak at best.

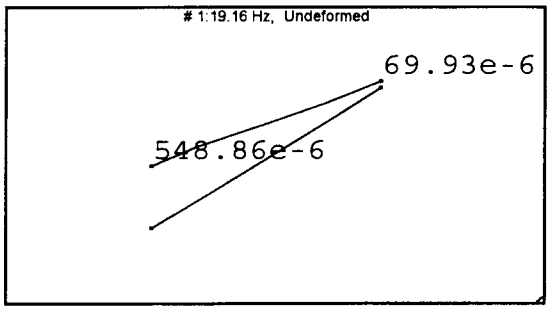

Figure 4-3. Mode 1, Config 1.

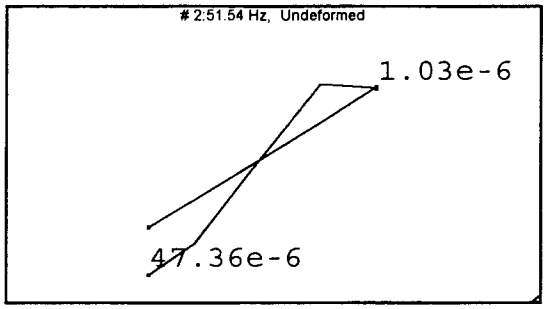

Figure 4-4. Mode 2, Config 1.

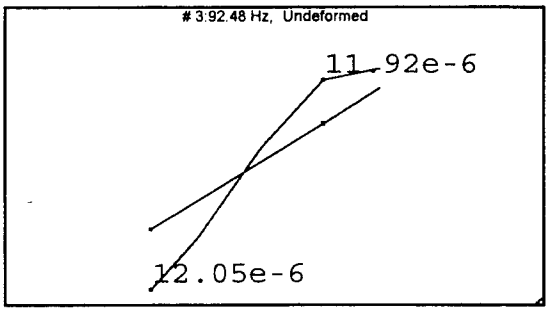

Figure 4-5. Mode 3, Config 1.

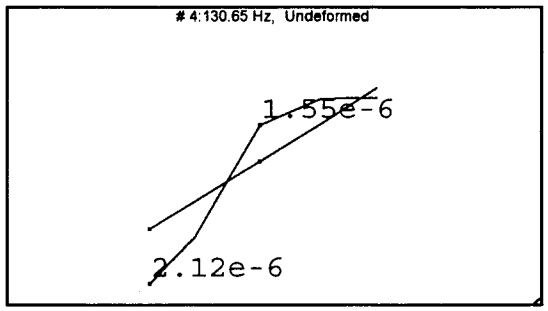

Figure 4-6. Mode 4, Config 1.

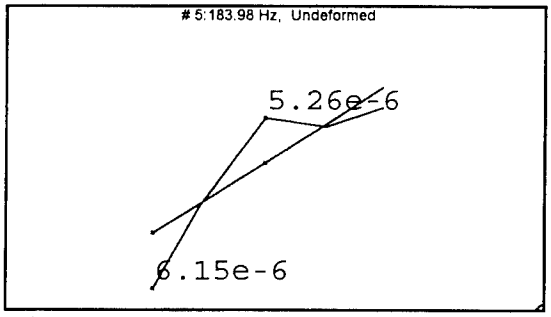

Figure 4-7. Mode 5, Config 1.

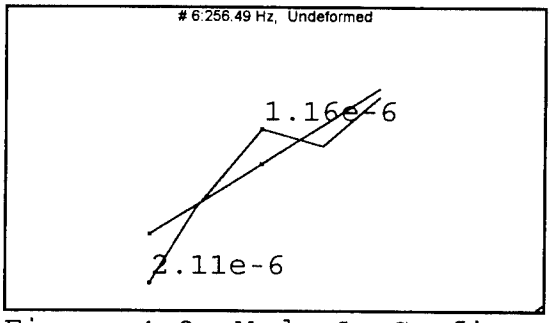

Figure 4-8. Mode 6, Config 1.

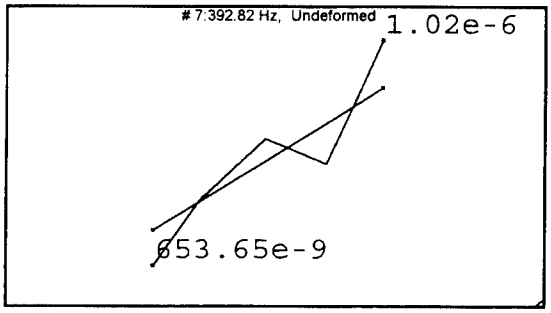

Figure 4-9. Mode 7, Config 1.

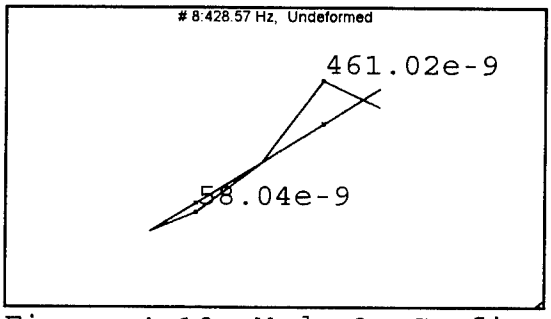

Figure 4-10. Mode 8, Config 1.

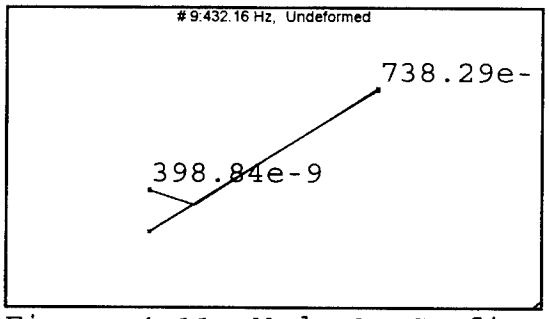

Figure 4-11. Mode 9, Config 1.

The first mode shape (Figure 4-3) is very similar to the fundamental shape for a clamped-free cantilever, with the stub rotor end of the barrel assembly not quite fixed, and the second mode shape (Figure 4-4) compares favorably to that of the first overtone of a clamped-free cantilever. The ratio of its frequency relative to the fundamental, however, does not compare; the second mode of a clamped-free bar has a frequency 6.3 times the fundamental. [Ref 13]

The motion of the gun barrel assembly for the second, third, and fourth modes is very nearly the same, yet their frequencies are quite different. It would be interesting to have measurements of the motion of other gun components for these modes as well, such as the gun housing. The motion of other elements could be distinguishing characteristics of mode shapes, as much as barrel assembly motion. This will be the subject of follow-on investigations.

E. MODAL SHAPES FOR CONFIGURATION WITH MUZZLE RESTRAINT

The mode shapes for configuration 5 are more numerous, and complex, than those for the unrestrained configurations. Thirteen modes below 500Hz were identified by STARModal. Again, some gun barrel assembly motion shapes were very similar for modes with quite different frequencies.

The fundamental mode (Figure 4-12) had the same shape as the other configurations, but was found at 24.7Hz vice 19.1Hz. It also only appeared once.

The second mode, at 84.5Hz, had a shape (Figure 4-13) that was very similar to the third mode shape for the other configurations and occurs at approximately the same frequency.

Other correspondences are more speculative. Mode 5 of the restrained configuration appears to correspond with mode 4 of the unrestrained configurations. Mode 10 of the restrained configuration appears to correspond to mode 6 of the unrestrained configurations.

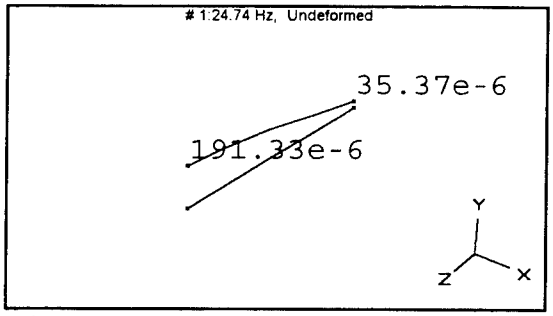

Figure 4-12. Mode 1, Config 5.

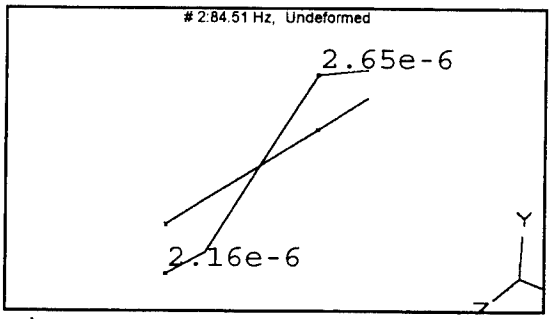

Figure 4-13. Mode 2, Config 5.

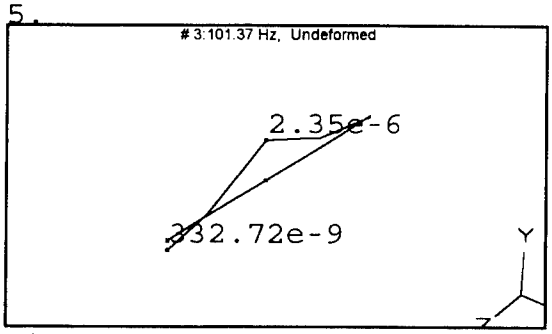

Figure 4-14. Mode 3, Config 5.

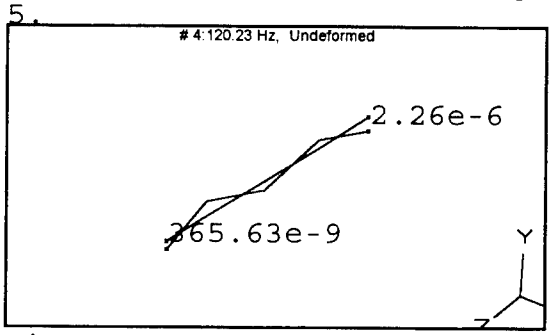

Figure 4-15. Mode 4, Config 5.

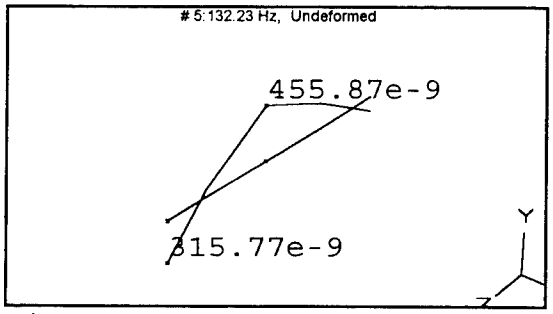

Figure 4-16. Mode 5, Config 5.

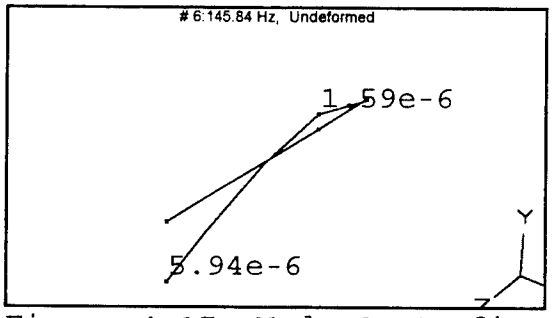

Figure 4-17. Mode 6, Config 5.

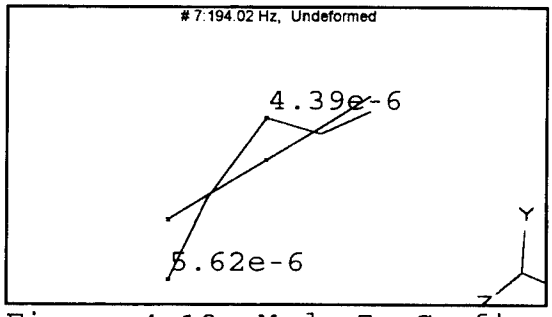

Figure 4-18. Mode 7, Config 5.

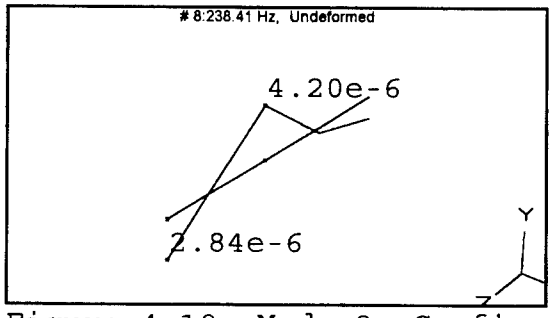

Figure 4-19. Mode 8, Config 5.

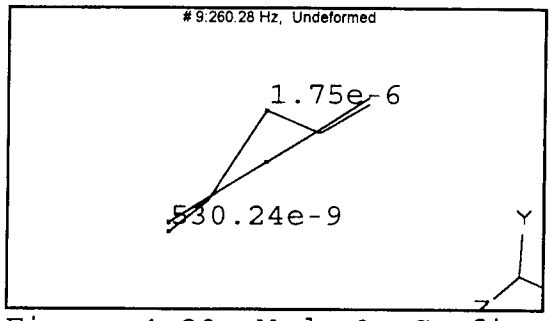

Figure 4-20. Mode 9, Config 5.

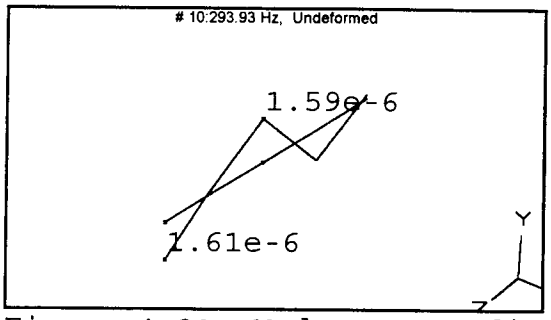

Figure 4-21. Mode 10, Config 5.

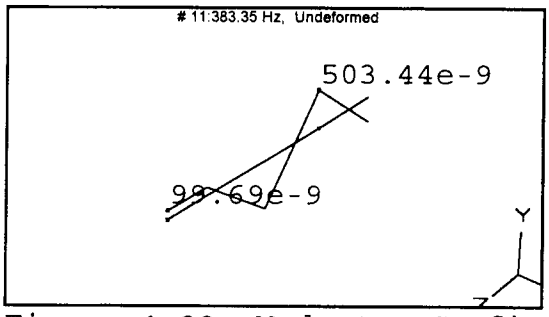

Figure 4-22. Mode 11, Config 5.

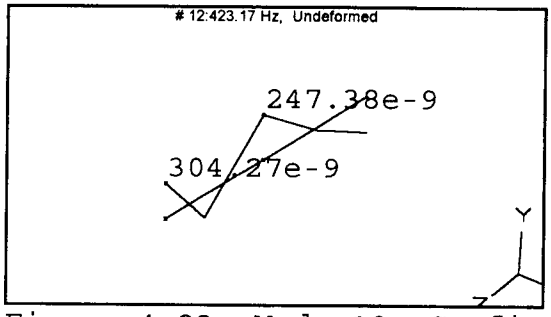

Figure 4-23. Mode 12, Config 5.

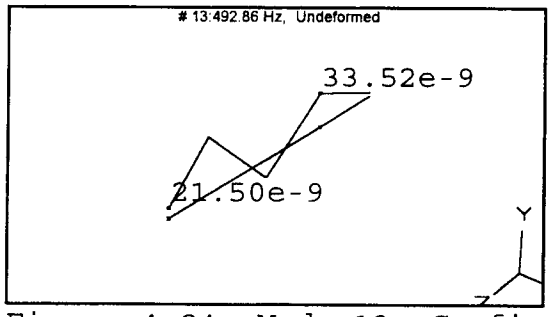

Figure 4-24. Mode 13, Config 5.

V. CONCLUSIONS

A. SUMMARY

A modal analysis of a PHALANX gun assembly was conducted in the laboratory at Naval Postgraduate School. The goal of this analysis is to provide a dynamical description of the gun for studies of the effects of gun modifications on bullet dispersion.

Accelerometer data were collected from five locations on the topmost barrel of the barrel assembly while the gun was being excited at the barrel tips with a swept sine forcing signal. This was done for five configurations of the gun, four of which did not include the production muzzle restraint, and the fifth that did. Frequency response data (vertical displacement/vertical force) were processed using the STARModal modal analysis software to extract modal parameters (frequencies, damping, and mode shapes) for frequencies up to 500Hz.

For the four unrestrained configurations, there were no major differences in FRF spectra, modal frequencies, or modal shapes. No more than nine modes were identified below 500Hz. For some modes the shape of the barrel assembly motion was very similar, suggesting that other structural responses might be present or that spatial aliasing due to the limited number of accelerometer locations influenced the determination of mode shapes at higher modal frequencies.

The fifth configuration, with muzzle restraint, was distinct from the others in all categories, generally displaying lower modal frequencies and a higher modal frequency density. Thirteen modes were identified below 500Hz for this configuration. Again, there was some repetition of barrel assembly shapes for different modes.

The muzzle restraint was designed to reduce barrel tip

vibration by the use of stiff members attached between a bearing collar and the gun cradle. A properly designed restraint would result in an increase of the modal frequencies. The results observed in this study show just the opposite for frequencies greater than about 125Hz. The barrel assembly with the muzzle restraint has a much higher modal density above this frequency. This result is significant, since it is known that the frequency spectrum of the forcing function of a firing bullet has significant amplitude above 125Hz. [Ref 14] Apparently, the stiffening effect provided by the bracing of the muzzle restraint is offset by the mass added by the muzzle restraint at the most reactive location of the barrel assembly, namely the barrel tips.

B. SUGGESTIONS FOR FOLLOW-ON INVESTIGATIONS

Using the system of accelerometers, recording analyzers, and STARModal software, as described in this thesis, the modal characteristics of the PHALANX gun have been successfully described, in a limited fashion. The system was relatively easy to implement and the modes identified agreed with rough calculations for similar structures. The following are some suggested improvements for follow-on investigations.

A more accurate picture of the mode shapes could be had if the number of degrees of freedom were increased. Time and equipment familiarity limited the number of excitation and measurement points in this study. STARModal supports up to 500 structural points as well as Cartesian, spherical, and cylindrical coordinates. This study could be expanded significantly to provide a better understanding of the modal characteristics of the PHALANX gun by including more measurement locations. This would reduce the repetition of mode shapes at different frequencies due to spatial aliasing.

The effect of non-linearities (i.e. "slop") is also an area of concern. The finite element model (FEM) is based upon

the assumption that at the location where the barrels mount into the stub rotor, the fit is "tight", allowing no motion. This may not be the case. During this study, it was discovered that the barrel assembly had some lateral free-play, even while under loaded conditions. The location of this free-play and its mechanism should be studied so that corrective adjustments could be incorporated into the FEM.

Independent testing of the modal response of the muzzle restraint is another suggestion. For frequencies above its fundamental frequency the stiffness of its arms becomes negligible, making it essentially a point mass. This would explain the modal response of configuration 5 and support the premise that the mass of the muzzle restraint has to be better distributed.

For this study, the gun was excited vertically at the center of the muzzle clamp. When a bullet is fired, actual excitation of the gun occurs collinear to the firing barrel along the firing barrel axis. Conducting a modal parameter study for this situation would provide some insight into the dynamical description of the gun under actual working conditions.

Once all laboratory studies have been completed, modal testing and live-fire vibration testing should be conducted in the field to see if the prominent mode frequencies appear in the vibration spectra for a firing gun. Of course, a real gun could not be loaded for FRF measurements, but loading is not believed to affect the modes very much.

The results of this study should be compared with those of the finite element model developed in references 3 and 4. The sources of any discrepancies between the two sets of results should be analyzed, quantified, and incorporated into the finite element model. This process will not only serve to

validate the finite element model, but will also provide a more accurate tool to predict the effects on bullet dispersion of potential modifications to the gun.

APPENDIX A. STARMODAL TUTORIAL

A. STARMODAL INITIALIZATION

Before introducing data into the STARModal software, a *Project Slate* has to be created to store the measurements that are to be analyzed. The data in each Project Slate should be restricted to measurements taken in one direction at whatever points that have been designated for the structure. To create this slate, go to Windows and click on the **SMS STAR System** icon in the **SMS Apps** window. Cancel the **Open** window that appears and either click on the **New Project** block in the Gateway path or in the **Project** pull-down menu. A window titled **New** should appear. This just creates a separate sub-directory for the Project Slate. Ensure that the directory that is to hold the project sub-directory is shown in the directory window and type the project name with the *.prj* extension in the **File Name** block. Click on **OK** to close the window.

The next block for modification is the **Project Slate** block itself. This block records a description of the data enclosed and some particulars of the experimental setup. The **Project ID** should reflect the file name (without the extension). The user enters any description that is applicable to the data in the file in the **Description** box. Under **Test Setup**, the appropriate method is clicked on and the DOF for the point of excitation is entered as described in the Structural Geometry section below. The **Measurement Units** box is self explanatory, with response determined by the type of sensor used to measure response; for accelerometers, the response is in m/s^2. The force measured by the impedance head was input as Newtons so, under **Excitation**, the designator scrolled to would be N. The last box to adjust is the **Analyzer** box. The appropriate analyzer model should be scrolled to (in this case HP35665) and the channels and address designators

ignored. They are to be used when transmitting data via the GPIB interface which is not covered in this tutorial. Click on OK and return to the Gateway path screen. Save the Project Slate by clicking on **Save** in the **Project** menu.

B. STRUCTURAL GEOMETRY

In order to view the modal shapes on the structure, a video facsimile of the structure has to be constructed. This facsimile is not an exact copy, but represents only those points where either measurements were taken or a force was applied. Any additional points included will only confuse the modal picture as they will appear to have no displacement, i.e. no measurements so no displacement associated. The measurement points are called degrees of freedom (DOF's) and have two components, a point number and a point direction. The point number is an arbitrarily assigned positive integer, starting from one (up to 500), that labels the point on the structure for which a particular measurement was taken. The point direction is a coordinate direction that relays the direction for which an accelerometer measurement or impedance head force was taken. The coordinate system used can be rectangular, spherical, or cylindrical.

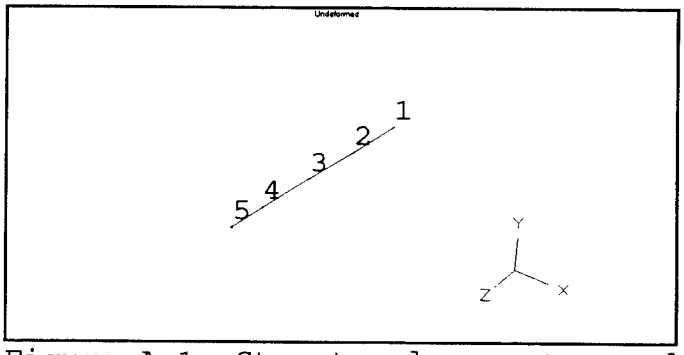

Figure A-1. Structural geometry and coordinate system used for PHALANX modal identification.

As an example, for the PHALANX, five points were used for data collection, one of which was also used to apply the force. Each point had a direction associated with it to denote the direction of measurement or excitation. For consistency with other concurrent studies (see Ref 14), the coordinate system used was rectangular and as depicted in Figure A-1. These points were more or less linearly arranged and all measurement was taken along the positive y-axis. This led to the use of a line structure composed of five interconnected points (Figure A-1). Though seemingly inadequate for demonstrating modal shapes for the more complex PHALANX, the simplicity reduced the number of data collection locations required as well as time for collection. The point numbers corresponded to accelerometer locations from the barrel end at the stub rotor (location/point 1) to the excitation point at the barrel tips (location/point 5) (Figure A-2).

Once the DOF points are identified, they have to be placed into tables so that STARModal can construct the model. The two tables required come up when, after opening the related Project Slate, the **Define Geometry** command is clicked on in either the Gateway path or the **Gateway** pull-down menu. They are labelled Coordinates and Display Sequence. The first records point information and the latter records the connections between the points to form the structure.

The Coordinates table has six columns. The first is the point number, which is automatically incremented from one on up to however many points are specified for the structure. These should match the point numbers used in disk translation and DOF designation. The next three columns are just the three coordinates that the point is assigned to in the structure's coordinate system, i.e. x, y, and z for rectangular, respectively. The fifth column, Component, is an arbitrary name that the user can specify to differentiate between different areas that groups of points belong to on a structure

(default is Main). And the last column is the coordinate system used, R for rectangular, S for spherical, and C for cylindrical. The Tab key can be used to go between each entry in the table. Whatever value is in the space below the File/Edit/Component row is the value that is inserted in the highlighted entry when tabbing through the entries. Save the table when complete.

Using the example of the PHALANX structure, there were five points designated (Table A-1). Coordinates #1 and #2 had no entries as the x- and y-coordinates were zero for these points.

Point #	Crd #1	Crd #2	Crd #3	Component	Type
1	0.00	0.00	54.0	Stub Rotr	R
2	0.00	0.00	90.0	Mid-Brl	R
3	0.00	0.00	126.0	Barrel	R
4	0.00	0.00	162.0	Mzl Clmp	R
5	0.00	0.00	185.0	Brl Tips	R

Table A-1. Coordinates Table example for PHALANX.

Coordinate #3 had values entered that corresponded to the distance of the accelerometer location from the back of the gun along the gun's, or z-, axis (in cm).

The next table that has to be completed is the Display Sequence table. The Coordinates table identified the points but did not connect the points to form a structure. The Display Sequence table establishes the lines between the points that will be deformed as the modal characteristics are applied. The Display Sequence table has four columns. The first identifies the line by a number in the same way that the

points are numbered. The next column is a Lift Pen option that, when any value is entered, goes to the start point designated without drawing a line. The Start Point column is where the first point in a line is put. The points have to correspond to point numbers in the Coordinates table. The End Point column is not required, but can be used to reduce the number of entries if a line connects many, consecutive points. Two start points designated with no entry for an end point will have a line drawn from the first to the second, without including any points that have values between the two, unless they coincidentally lie on the line between the two designated points.

Again, using the PHALANX model as an example, five lines are listed (Table A-2). The pen is lifted at the first point

Line #	Lift Pen	Start Pt	End Pt
1	X	1	
2		2	
3		3	
4		4	
5		5	

Table A-2. Display Sequence table example for PHALANX.

(recommended by the software) and the start points are listed in order. This creates lines that connect the points in the order listed. The same result could arise by having one line that has point #1 as the start point and point #5 as the end point. Save the table when complete.

Completion of the Coordinates and Display Sequence tables automatically sets up the animation figure. To validate the structure of the model, click on the **Show Structure** command in either the Gateway path or the **Gateway** pull-down menu. Two windows will appear. The one on the left with the structure figure and a coordinate system representation is the animation window. The long one on the right is the **View Control** window. It allows manipulation of the animation figure. When data has been processed in the Project Slate, the modal shapes and their motion will be displayed in the animation window.

The mode shape animation is composed of forty-eight still frames that are displayed in a continuous cycle. In the animation window are two menus, **Edit** and **Animation**. The **Edit** menu has a **Still/Copy/Print** command that allows the user to pick any number of frames, freeze them, and send the multiple exposure image to a printer. Single mode shapes can be handled in the same manner. The **Animation** menu allows a choice of time-domain or frequency domain animation and provides for the numbering of the points or assignment of results' values to the points of the structure. This is done with the **Highlight** command. The designation of points is controlled by the user, options being the highlighting of a single point, pairs of points or a range of points. [Ref 12]

The **View Control** dialog box has four primary sections: Source, Type, Adjustments, and Orientation. The Source section allows a choice of two traces, A or B, to be displayed in the animation window. Below this is a drop-down list of three states for the traces: Results, Deformation, or Undeformed. Results displays the shape of the mode specified in the mode number box. If Deformation is chosen, the shape will reflect data that is the result of the Forced Response Simulation option in the SMS. The Undeformed state displays the structure with no deformation so the deformed states can be compared to the unexcited structure. [Ref 12]

The Type section allows a choice of display options. The screen can be either a full screen for one trace (Full), overlapped traces (Front/Back), or side-by-side traces (Split). The modal shapes can be viewed as vectors that change length with the modal frequency, or as sinusoidal deformations of the structure (Contour). The last option changes trace from Normal to Complex results displayed. [Ref 12]

The Adjustments section allows for the manipulation of several parameters that affect the animation of the traces. Perspective changes the viewing distance from the structure. Its values range from 0-100, 0 corresponding to a viewing distance of infinity, and 100 the closest possible viewing distance. Although the amplitude displayed has no relation to the actual amplitude of the structure's response, the relative amplitudes between points of the structure are indicative of relative motion between the points for the particular mode displayed. Adjusting the amplitudes using the Amplitude control increases or decreases the amplitudes of the trace. Its limits are 0 and 100, where 0 is no amplitude and 100 is maximum. The Zoom control acts like a magnifier of the entire animation window. And, the Speed control changes the rate of cycling through the animation frames. [Ref 12]

The Orientation section is used to manipulate the viewing angle of the structure. Changing the values at any of the coordinates amounts to rotating about the axis specified. Marking the Auto box results in continuous rotation about the designated axis.

C. DISK TRANSLATION

The import of actual FRF measurements can be done in one of two ways. The first, for which the user is referred to the SMS literature, is via GPIB interface between analyzer and STARModal machine. The second, which was the method used for this study, is import on disk.

The mechanism for the import of analyzer files to STARModal is the STAR Data Disk Translator, a utility program that reads measurements stored in an analyzer's native format and then translates that into a format compatible with the STAR system. This allows field measurements without the burden of transporting the computer that houses STARModal. Analysis of measurements can wait until the analyzer measurements, stored on disk, can be returned to the laboratory.

To run the disk translator, first insert the disk with the data into the machine running STARModal. Go to Windows and click on the **Disk Translator** icon in the **SMS Apps** box. This brings up the **STAR Data Disk Translator** window. In the **Analyzer** menu, click on the analyzer from which the data was stored. Select Manual in the **DOF Labelling Method** box. Now, the source and destination have to be identified.

Click on the **Source Directory** box to bring up the corresponding window. Change source directory to "a:" and click on OK, this should change all the source files to those on the disk.

Now, bring up the destination directory the same way. Click through the directory path until the Project Slate directory appears in the **Destination Directory** box. It should look something like "c:..\(directory name)." All measurements translated during this transaction will be stored in the destination directory.

Now, each of the measurement files has to be renamed in order to comply with the STARModal software. The procedure consists of highlighting the file to be translated in the **Source File** box and stipulating the DOF's for the file. Highlighting the file causes the file name to title the previously named No File Selected box. Two entries, "Chan. 1:" and "Chan. 2:," will also appear. They will both be marked as undefined. Use the scrolling controls to enter point and direction of measurements that each channel represents. These

points must correspond to the point numbers in the animation figure.

For PHALANX, channel one was the force measurement and channel two was the accelerometer measurement. The force, always applied at the end of the muzzle clamp in the positive y direction, was labelled 5Y. This was entered for the channel one entries. The five represents the fifth point in the animation figure and Y the direction of excitation. Channel two had one of five entries depending upon the point where the accelerometer was placed for measurement. This resulted in labels of 1Y, 2Y, 3Y, 4Y, and 5Y.

After entering the DOF for the file, click on add and the file name appears in the **Files to Translate** box and the **DOF List** box. The latter also displays the DOF's entered for the file. The procedure is repeated for all files that are to be assembled from the current project slate.

Once all files have had DOF's assigned, click on the Translate icon and translation will commence revealing an indicator that tells how much of the data has been translated. When 100% is annotated, click on OK in the **Data Translation Complete** box and close the **Star Data Disk Translator** window.

D. FRF ANALYSIS

Once the measurements have been made readable by the disk translator, they are ready for processing. First, all extraneous data that may be present from a previous session needs to be cleared from SMS data tables. Starting from the **Project Slate** window, go to the **Tables** menu and click on Clear. Then highlight Autofit and click on Clear icon. Do the same for the Frequency Results and Time Results entries. This must be done every time that a curve fit is executed.

The next step is to identify the modes and the frequencies where they occur in the data set. Click on Modal Peaks in the **Analysis** pull-down menu. This brings up the **Modal**

Peaks to Block 2 window. The entry for the Measurement File should match the file of the data set being analyzed. The point range can be specified or All selected. This uses the point values in the current coordinate table. For the PHALANX measurements, a point range of 1 to 5 and direction of Y was specified. If the point range or directions are over specified, the modal peaks function will skip measurements which are within the specified range but not available in the translated files. The Magnitude^2 calculation method was selected because the modal peaks were visually identified by looking at the magnitude of the FRF traces. Click on **OK** to close the window.

Now, the curve fitting bands are ready to be established. Curve fitting is the process used to identify the modal parameters that will be used to animate the structure model. To get to the **Measurement** and **Curve Fit** windows, click on Identify Modes in either the **Gateway** or **Analysis** menus. Both windows appear simultaneously.

The **Measurement** window is used to frame the modal peaks between measurement cursor bands for curve fitting. The window has two trace blocks, Block 1 and Block 2. The contents of each can be controlled by the Trace and Axes menus, the former handles which block is visible and active, while the latter determines the coordinates of the active block. Block 2 holds the trace that corresponds to the STARModal identified modal peaks as mentioned above. Block 1 is used to open the file that best presents the modal information. The trace used should have sharp peaks at the modes and sharp delineation between modes. Check all the files in the data set by opening each and comparing them to the Block 2 trace. Once a trace is chosen, leave it in the window on Block 1. It may be beneficial to try different axes units, i.e. real, imaginary, etc..., to further enhance modal identification.

The **Curve Fit Panel** controls the actual curve fit

process. Pick a curve fit method from the choices at the left of the panel. The STAR Reference Manual gives a good description and purpose for each. On the right of the panel x in all the boxes that apply (it doesn't hurt to mark them all). Go to No. of Modes and click on the arrows until 1 appears. Now go back to Measurement window and click on the first modal peak. A cursor will appear at that peak. If desired, the cursor can be split about the peak to make a curve fit band. For polynomial curve fitting the band will automatically be set if not pre-designated. Return to the curve fit panel and insure that the band number is 1, then click on the Fit icon. Repeat the procedure for the rest of the peaks, incrementing the band number each time (and nothing else). Once all peaks have been fit, x in the Autofit box and click on the Fit icon. This brings up an **Auto Fit Preferences** window that should be completed similarly to the **Modal Peaks to Block 2** window.

Once the Autofit is completed, close the **Freq Response** and **Curve Fit Panel** windows. Then click on the Show Structure block in the Gateway path or on the Gateway menu to bring up the animation viewing window. The first mode will be displayed with vector displacements. Use the tools described in Section B of this appendix to manipulate the figure and print out the results.

APPENDIX B. ANALYZER INPUT AND MEASUREMENT STATES

The input and measurement states of the HP 35665A analyzer used in this investigation are included to facilitate replication of the experiment. The measurement state includes the excitation characteristics as well as the analyzer display layout. Note, on the Meas Data line, the Data A trace shows F2. This is a reference to function 2 on the analyzer which was set to divide the acceleration FRF by $(j\omega)^2$ to convert to a displacement FRF.

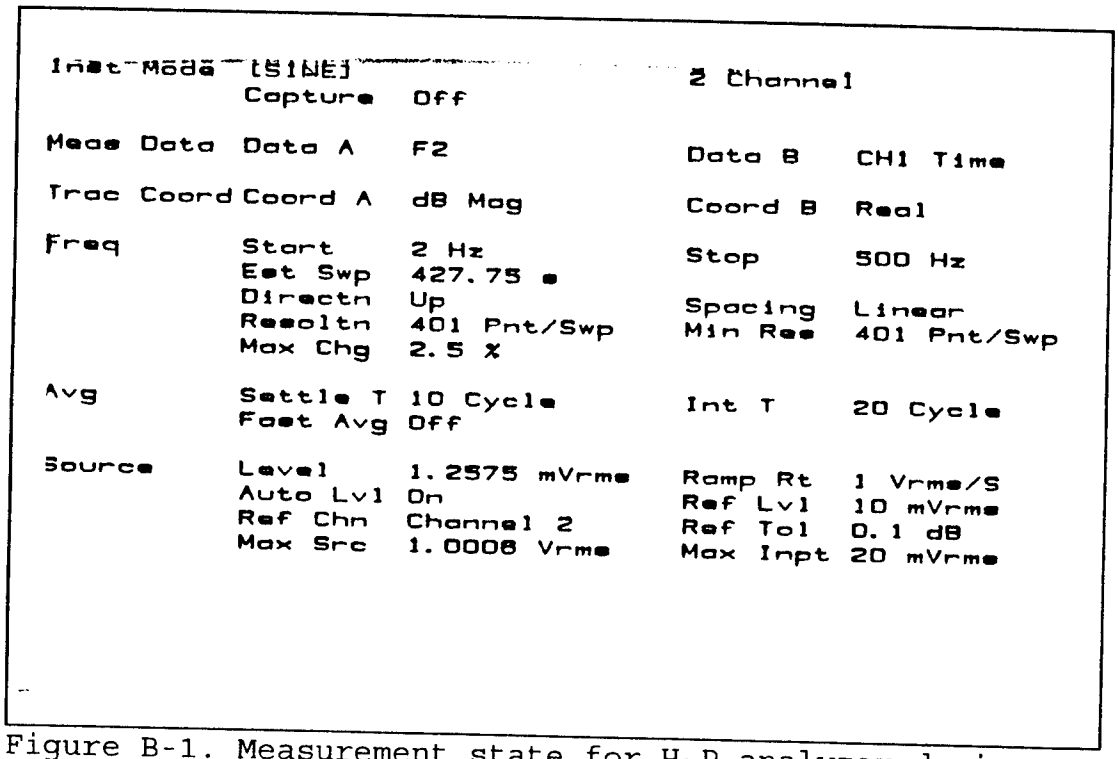

Figure B-1. Measurement state for H-P analyzer during data collection.

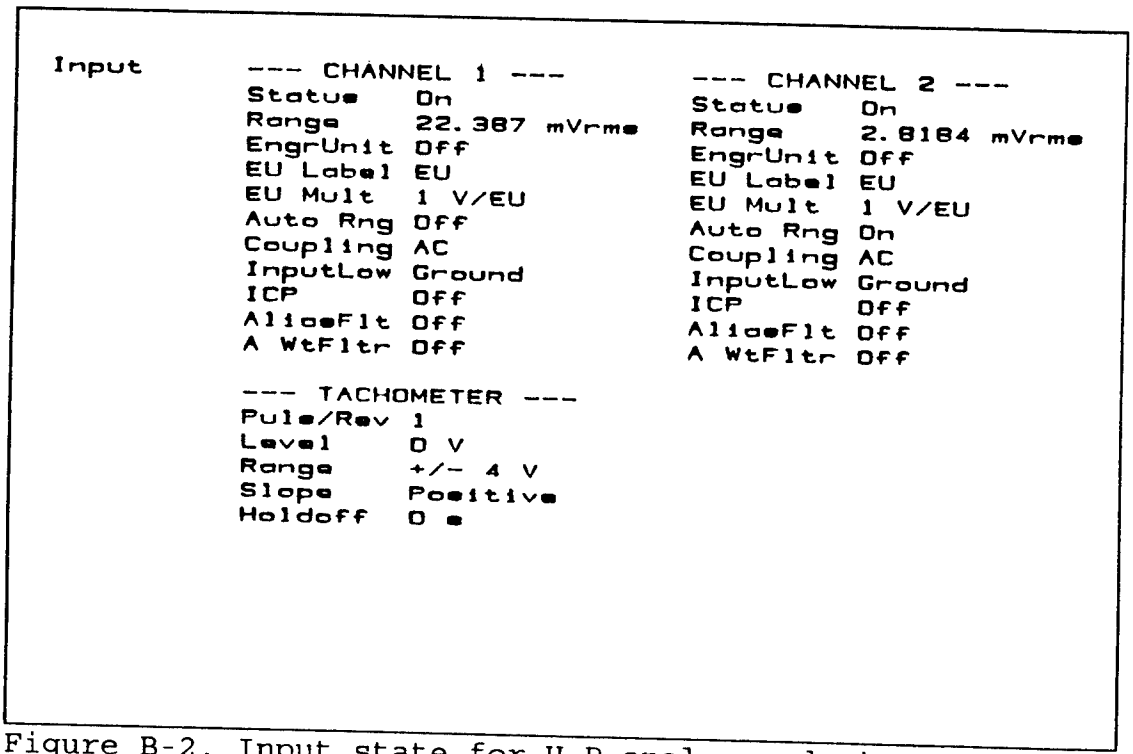

Figure B-2. Input state for H-P analyzer during data collection.

APPENDIX C. FREQUENCY RESPONSE FUNCTIONS FOR ACCELEROMETER LOCATION 1

Figure C-1 shows the frequency response function (FRF) (vertical displacement/vertical force) measured at accelerometer location 1 for the five configurations. Table C-1 lists the resonance peak frequencies which were manually identified from the FRF's off the screen of the H-P signal analyzer.

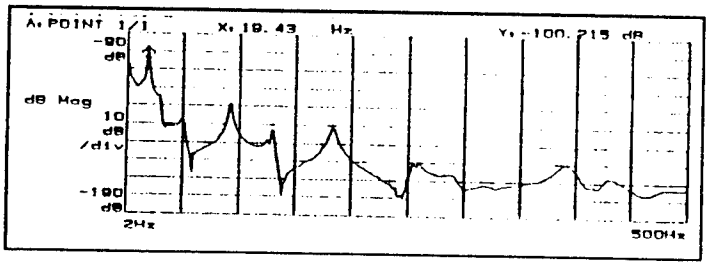

Config 1

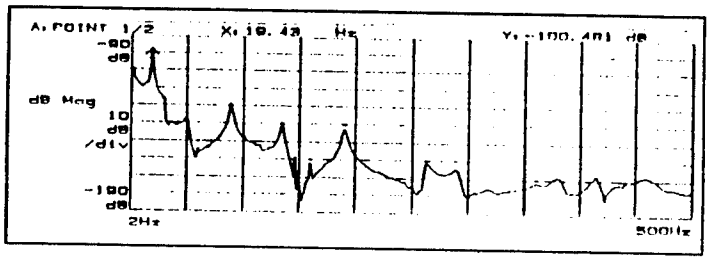

Config 2

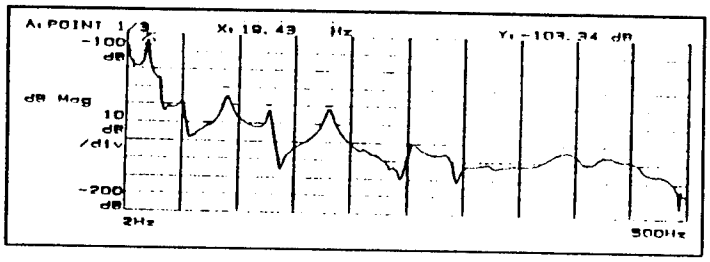

Config 3

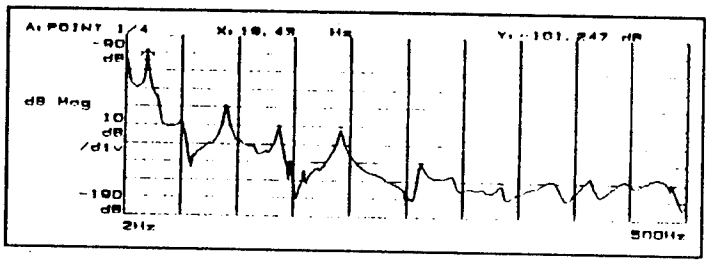

Config 4

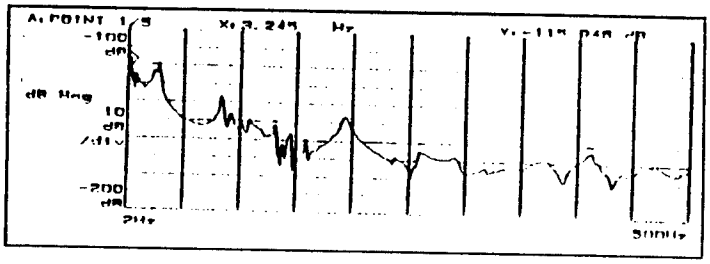

Config 5

Figure C-1. FRF's recorded at accelerometer location 1.

		CONFIG 1	CONFIG 2	CONFIG 3	CONFIG 4	CONFIG 5
1						3.245
2		19.43	19.43	19.43	19.43	
3						28.145
4		49.31	49.31	49.31	49.31	
5						84.17
6		92.885	89.15	90.395	89.15	92.885
7						101.6
8						109.07
9		130.235	135.215	127.745	136.46	131.48
10						145.175
11			160.115			158.87
12		183.77	189.995	180.035	191.24	193.73
13		259.715	263.45	255.98	263.45	260.96
14			289.595			
15					334.415	318.23
16			379.235		377.99	370.52
17		390.44		392.93		
18			414.095		414.095	412.85
19		429.035		425.3		
20					445.22	441.485
21						458.915

Table C-1. Resonance peak frequencies for accelerometer location 1.

APPENDIX D. FREQUENCY RESPONSE FUNCTIONS FOR ACCELEROMETER LOCATION 2

Figure D-1 shows the frequency response function (FRF) (vertical displacement/vertical force) measured at accelerometer location 2 for the five configurations. Table D-1 lists the resonance peak frequencies which were manually identified from the FRF's off the screen of the H-P signal analyzer.

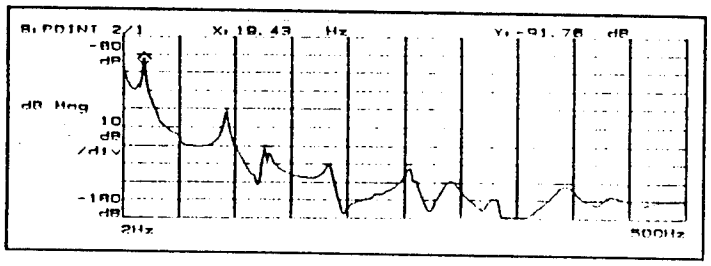

Config 1

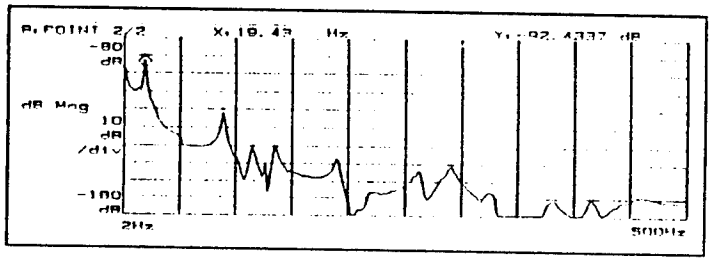

Config 2

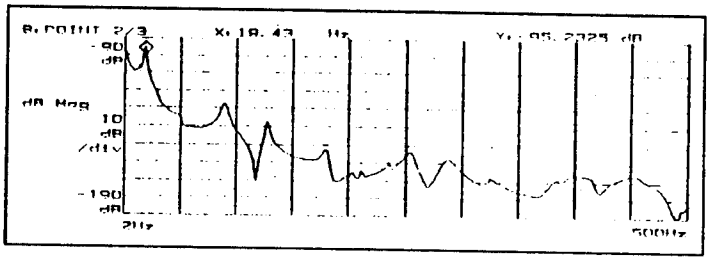

Config 3

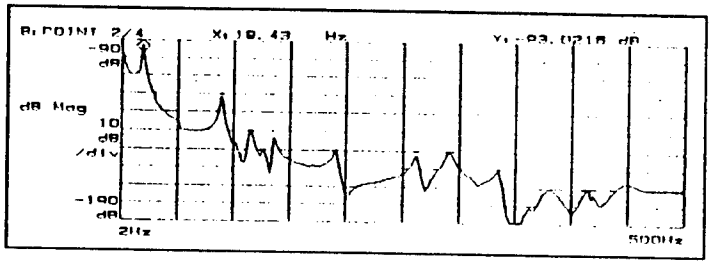

Config 4

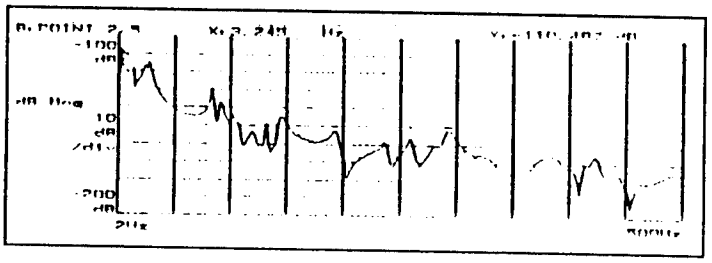

Config 5

Figure D-1. FRF's recorded at accelerometer location 2.

		CONFIG 1	CONFIG 2	CONFIG 3	CONFIG 4	CONFIG 5
1						3.245
2						14.45
3		19.43	19.43	19.43	19.43	
4						28.145
5						84.17
6		92.885	89.15	89.15	89.15	91.64
7					115.295	120.275
8		126.5	135.215	127.745	136.46	132.725
9						145.175
10		183.77	189.995	178.79	191.24	192.485
11						236.06
12		254.735	262.205	253.49	262.205	259.715
13		292.085	290.84	287.105	292.085	293.33
14		329.435	324.455	325.7	334.415	
15		391.685	380.48	399.155	379.235	382.97
16		432.77	415.34		414.095	422.81
17				448.955	445.22	438.975

Table D-1. Resonance peak frequencies for accelerometer location 2.

APPENDIX E. FREQUENCY RESPONSE FUNCTIONS FOR ACCELEROMETER LOCATION 3

Figure E-1 shows the frequency response function (FRF) (vertical displacement/vertical force) measured at accelerometer location 3 for the five configurations. Table E-1 lists the resonance peak frequencies which were manually identified from the FRF's off the screen of the H-P signal analyzer.

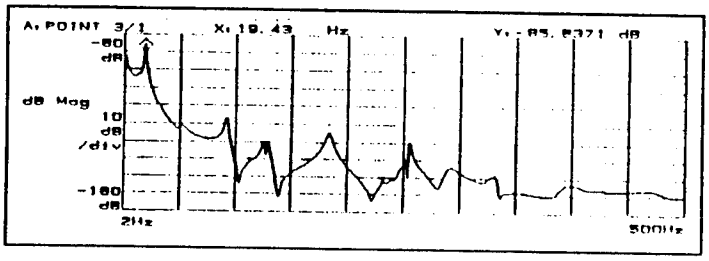

Config 1

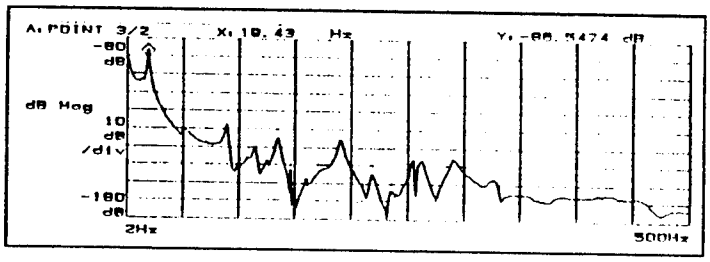

Config 2

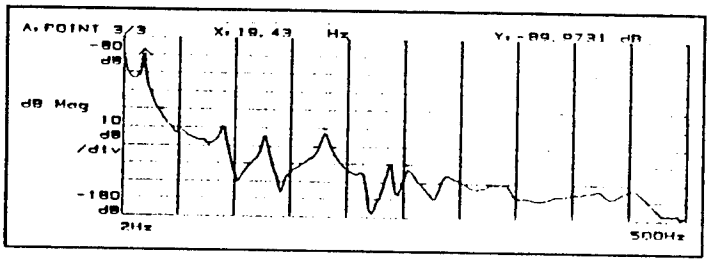

Config 3

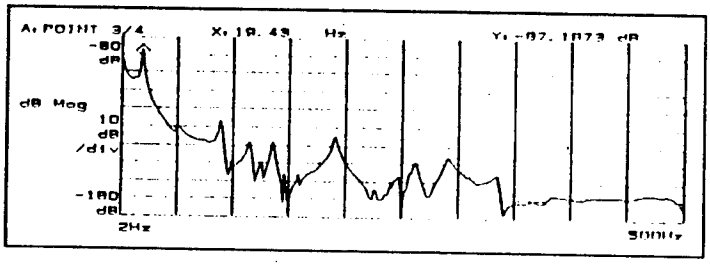

Config 4

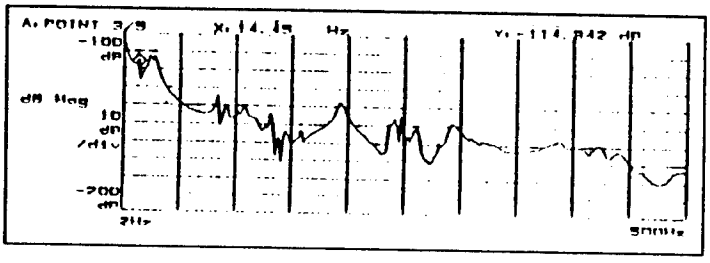

Config 5

Figure E-1. FRF's recorded at accelerometer location 3.

		CONFIG 1	CONFIG 2	CONFIG 3	CONFIG 4	CONFIG 5
1						14.45
2		19.43	19.43	19.43	19.43	
3						24.41
4			50.555	50.555	51.8	
5						84.17
6		92.885	89.15	89.15	89.15	91.64
7						107.825
8			114.05		115.295	
9		126.5		126.5	125.255	
10			135.215		136.46	131.48
11						145.175
12						158.87
13		183.77	189.995	180.035	191.24	193.73
14			218.65	238.55		242.285
15		254.735	253.98	254.735	247.265	248.51
16			263.45		263.45	260.96
17		292.085	290.84	288.35	292.085	294.575
18		329.435	325.7		334.415	
19		391.685				386.705
20		432.77		422.81		421.565
21				451.445		438.995

Table E-1. Resonance peak frequencies for accelerometer location 3.

APPENDIX F. FREQUENCY RESPONSE FUNCTIONS FOR ACCELEROMETER LOCATION 4

Figure F-1 shows the frequency response function (FRF) (vertical displacement/vertical force) measured at accelerometer location 4 for the five configurations. Table F-1 lists the resonance peak frequencies which were manually identified from the FRF's off the screen of the H-P signal analyzer.

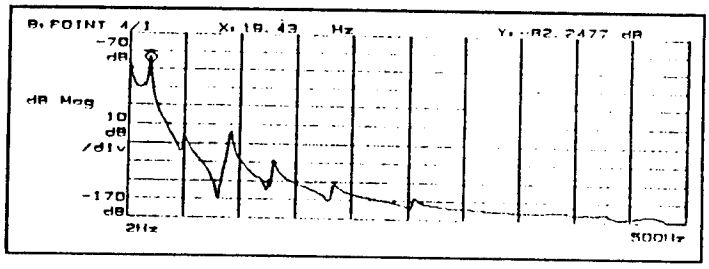

Config 1

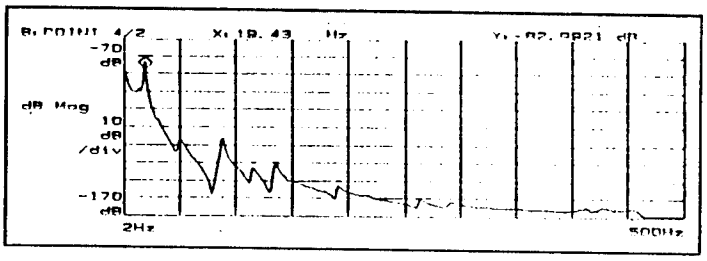

Config 2

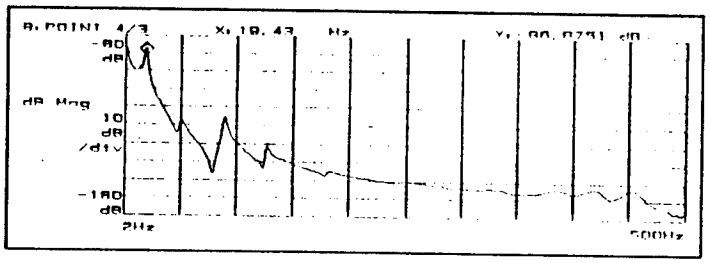

Config 3

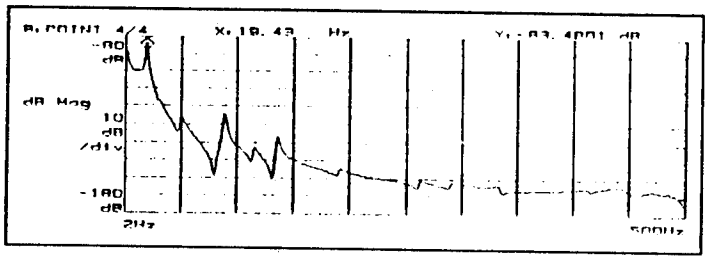

Config 4

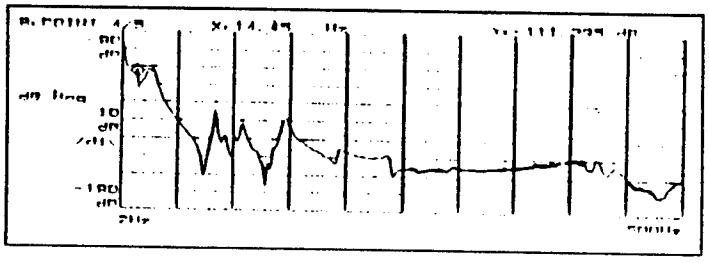

Config 5

Figure F-1. FRF's recorded at accelerometer location 4.

		CONFIG 1	CONFIG 2	CONFIG 3	CONFIG 4	CONFIG 5
1						14.45
2		19.43	19.43	19.43	19.43	
3						25.655
4		50.555	50.555	50.555	50.555	
5						84.17
6		92.885	87.905	90.395	89.15	
7						109.07
8			115.295		116.54	
9				127.745		
10		130.235	135.215		136.46	
11						147.665
12		185.015	191.24	182.525	191.24	194.975
13						236.06
14		257.225	264.695		264.695	
15					293.33	
16				420.32		424.055
17				451.445		440.24

Figure F-1. Resonance peak frequencies for accelerometer location 4.

APPENDIX G. FREQUENCY RESPONSE FUNCTIONS FOR ACCELEROMETER LOCATION 5

Figure G-1 shows the frequency response function (FRF) (vertical displacement/vertical force) measured at accelerometer location 5 for the five configurations. Table G-1 lists the resonance peak frequencies which were manually identified from the FRF's off the screen of the H-P signal analyzer.

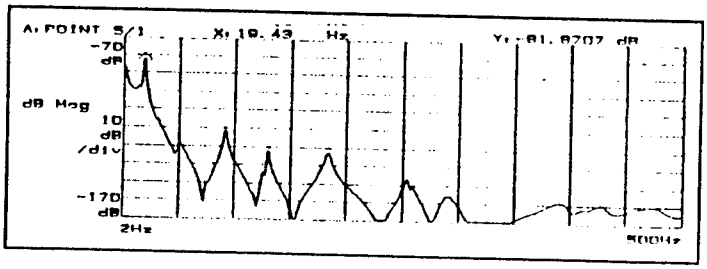

Config 1

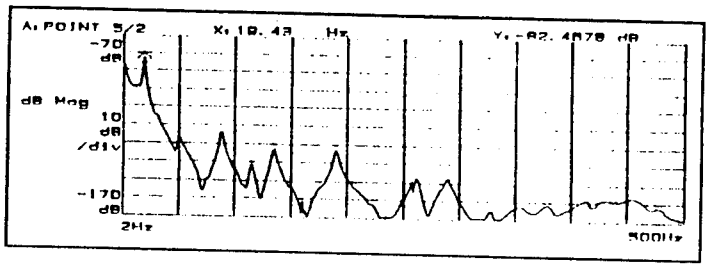

Config 2

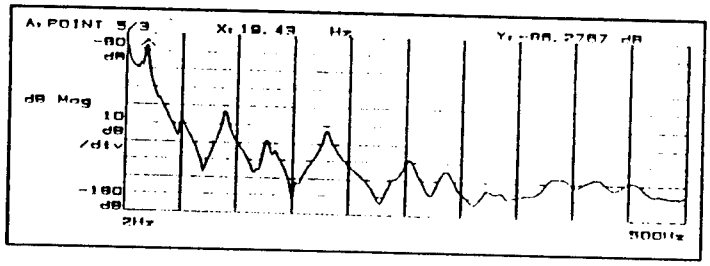

Config 3

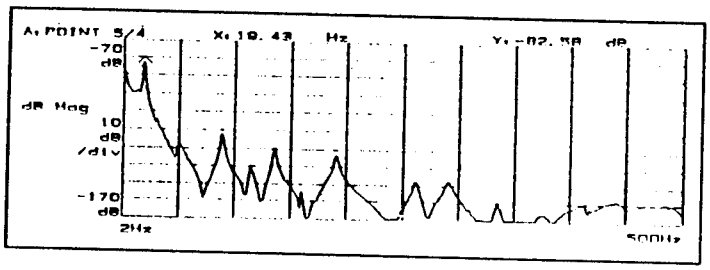

Config 4

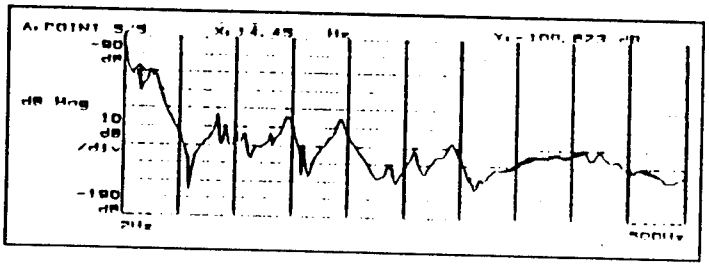

Config 5

Figure G-1. FRF's recorded at accelerometer location 5.

		CONFIG 1	CONFIG 2	CONFIG 3	CONFIG 4	CONFIG 5
1						14.45
2		19.43	19.43	19.43	19.43	
3						24.41
4		50.555	50.555	50.555	50.555	
5						84.17
6		91.64	87.905	89.15	89.15	91.64
7						101.6
8						107.825
9			115.295		115.295	
10				126.5		
11		130.235	135.215		136.46	
12						146.42
13		183.77	189.995	180.035	191.24	193.73
14						237.305
15		254.735		253.49		
16			262.205		262.205	259.715
17		289.595	289.595	285.86	290.84	293.33
18			328.19	323.21	335.66	
19			354.555			
20		389.195	379.235	381.725	377.99	
21						404.135
22			412.85	420.32		424.055
23				451.445		440.24

Table G-1. Resonance peak frequencies for accelerometer location 5.

APPENDIX H. MODAL SHAPES FOR CONFIGURATION 1

Gun configuration 1 had the topmost barrel at top dead center, no muzzle restraint, and no load upon the stub rotor.

STARModal identified nine modes (Figures 4-3 to 4-11 in Chapter IV) in the 2-500Hz excitation range for this configuration. The numbers on the shapes are relative displacements between the corresponding points on the shape. No other connotation should be attributed to them.

Table H-1 lists the amplitudes and phase angles computed by STARModal for configuration 1.

MODE	Accelerometer Location	Amplitude	Phase Angle
1	1	69.93e-6	-81.57
	2	190.30e-6	-84.27
	3	350.42e-6	-85.08
	4	499.86e-6	-86.34
	5	548.86e-6	-87.08
2	1	1.03e-6	16.68
	2	31.55e-6	-98.40
	3	35.87e-6	-171.34
	4	39.78e-6	139.99
	5	47.36e-6	146.64
3	1	5.10e-6	121.04
	2	11.92e-6	118.51
	3	4.69e-6	109.74
	4	6.73e-6	-19.46
	5	12.05e-6	-49.72
4	1	600.44e-9	-80.28
	2	921.95e-9	149.87
	3	1.55e-6	121.16
	4	1.14e-6	-32.51
	5	2.12e-6	-59.18
5	1	2.50e-6	-40.68
	2	538.61e-9	-73.40
	3	5.26e-6	140.73
	4	1.68e-6	79.68
	5	6.15e-6	-37.66

Table H-1. Amplitudes and phases computed by STARModal for configuration 1.

MODE	Accelerometer Location	Amplitude	Phase Angle
6	1	287.67e-9	-12.91
	2	1.16e-6	-73.41
	3	1.16e-6	150.84
	4	191.31e-9	-91.12
	5	2.11e-6	-63.37
7	1	1.02e-6	163.90
	2	815.78e-9	-20.55
	3	449.71e-9	162.60
	4	33.24e-9	103.54
	5	653.65e-9	-18.85
8	1	135.88e-9	-163.09
	2	461.02e-9	-11.65
	3	4.88e-9	-35.34
	4	58.04e-9	-158.99
	5	391.48e-12	124.24
9	1	738.29e-12	-163.87
	2	52.23e-12	127.26
	3	328.33e-12	-41.58
	4	1.15e-9	-160.89
	5	398.84e-9	-92.83

Table H-1 (cont.).

APPENDIX I. MODAL SHAPES FOR CONFIGURATION 2

Gun configuration 2 had the topmost barrel at top dead center, no muzzle restraint, and a static load pulling back on the stub rotor to simulate the maximum load experienced during firing.

STARModal identified seven modes (Figures I-1 to I-7) in the 2-500 Hz excitation range for this configuration. The numbers on the shapes are relative displacements between the corresponding points on the shape. No other connotation should be attributed to them.

Table I-1 lists the amplitudes and phase angles computed by STARModal for configuration 2.

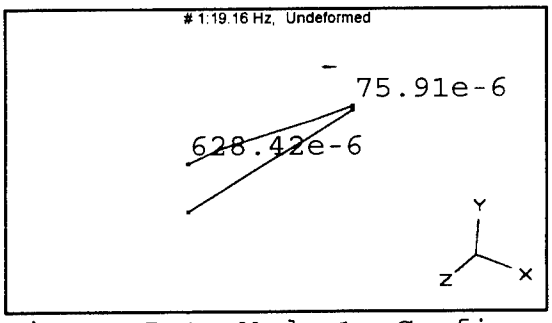

Figure I-1. Mode 1, Config 2.

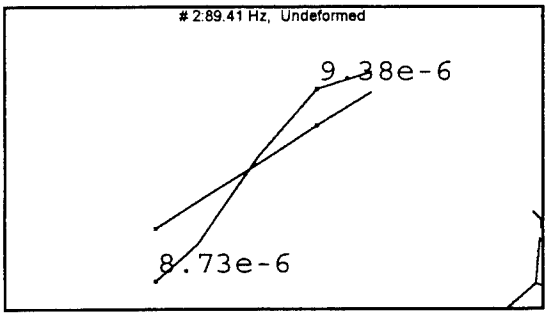

Figure I-2. Mode 2, Config 2.

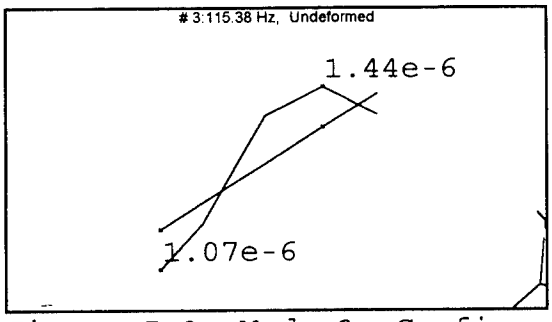

Figure I-3. Mode 3, Config 2.

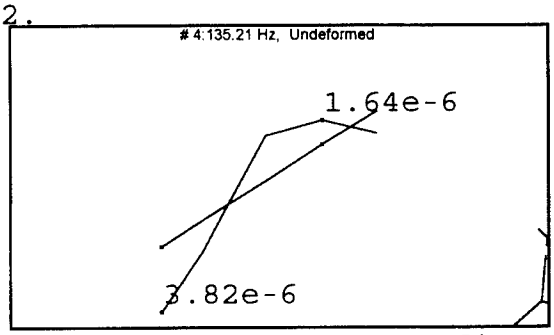

Figure I-4. Mode 4, Config 2.

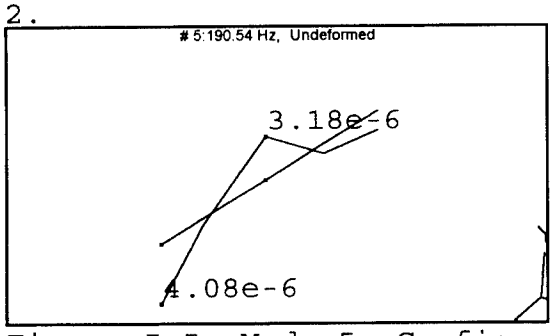

Figure I-5. Mode 5, Config 2.

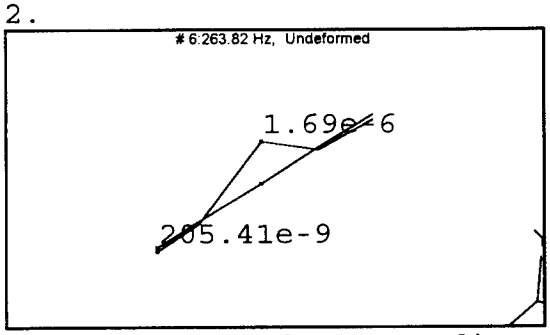

Figure I-6. Mode 6, Config 2.

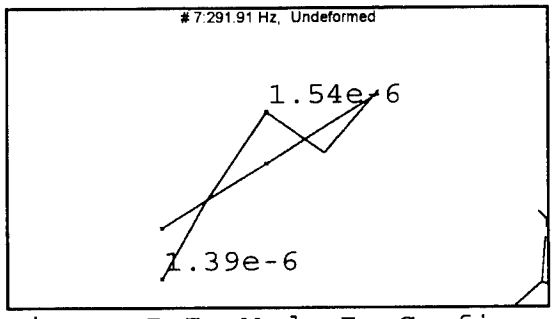

Figure I-7. Mode 7, Config 2.

MODE	Accelerometer Location	Amplitude	Phase Angle
1	1	75.91e-6	-81.87
	2	209.81e-6	-80.79
	3	394.19e-6	-81.03
	4	572.02e-6	-82.46
	5	628.42e-6	-82.71
2	1	4.84e-6	122.48
	2	9.38e-6	118.54
	3	1.72e-6	129.12
	4	6.42e-6	5.45
	5	8.73e-6	-37.59
3	1	607.84e-9	-7.43
	2	1.44e-6	124.10
	3	1.65e-6	121.88
	4	535.43e-9	-22.81
	5	1.07e-6	-42.00
4	1	1.46e-6	-42.87
	2	1.64e-6	124.54
	3	2.88e-6	138.48
	4	1.91e-6	-72.21
	5	3.82e-6	-51.89
5	1	1.48e-6	-34.47
	2	785.44e-9	-38.81
	3	3.18e-6	144.14
	4	402.45e-9	17.27
	5	4.08e-6	-33.34

Table I-1. Amplitudes and phases computed by STARModal for configuration 2.

MODE	Accelerometer Location	Amplitude	Phase Angle
6	1	148.12e-9	-15.03
	2	89.33e-9	-46.47
	3	1.69e-6	-137.91
	4	65.86e-9	14.76
	5	205.41e-9	-72.74
7	1	119.17e-9	133.64
	2	848.11e-9	-50.60
	3	1.54e-6	138.94
	4	69.50e-9	23.37
	5	1.39e-6	-43.68

Table I-1 (cont.).

APPENDIX J. MODAL SHAPES FOR CONFIGURATION 3

Gun configuration 3 had the uppermost barrel in firing position, no muzzle restraint, and no load upon the stub rotor.

STARModal identified eight modes (Figures J-1 to J-8)in the 2-500 Hz excitation range for this configuration. The numbers on the shapes are relative displacements between the corresponding points on the shape. No other connotation should be attributed to them.

Table J-1 lists the amplitudes and phase angles computed by STARModal for configuration 3.

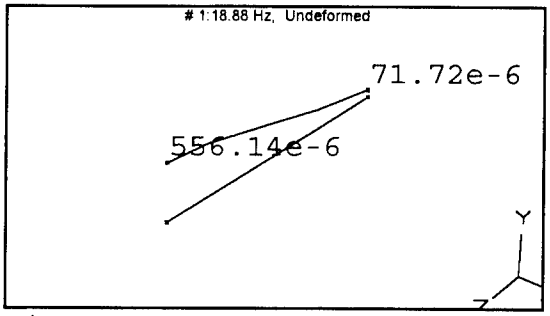

Figure J-1. Mode 1, Config 3.

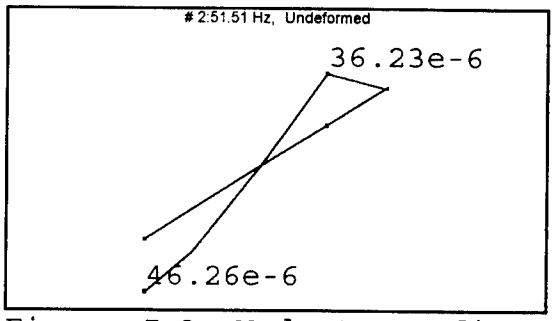

Figure J-2. Mode 2, Config 3.

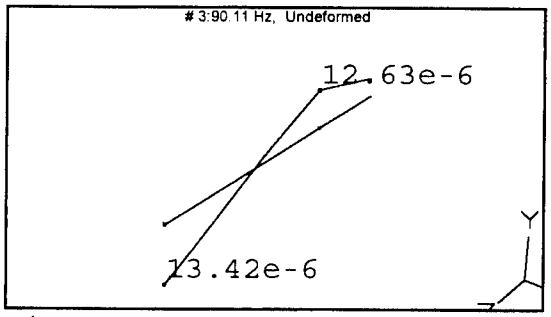

Figure J-3. Mode 3, Config 3.

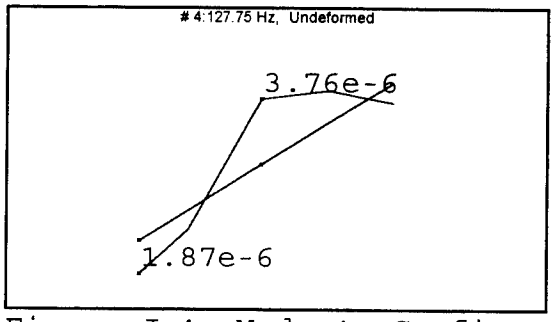

Figure J-4. Mode 4, Config 3.

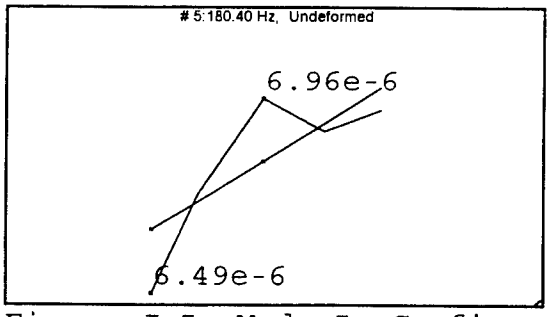

Figure J-5. Mode 5, Config 3.

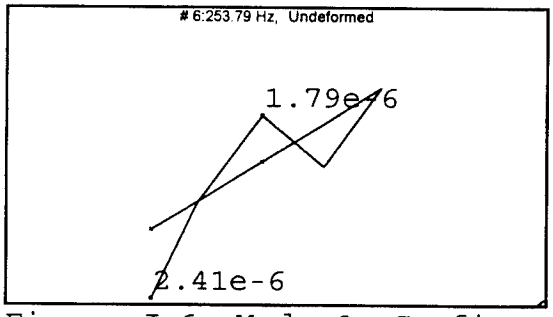

Figure J-6. Mode 6, Config 3.

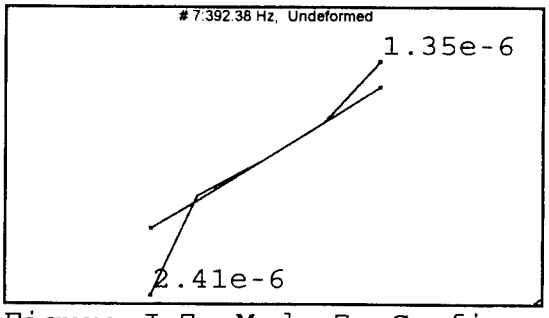

Figure J-7. Mode 7, Config 3.

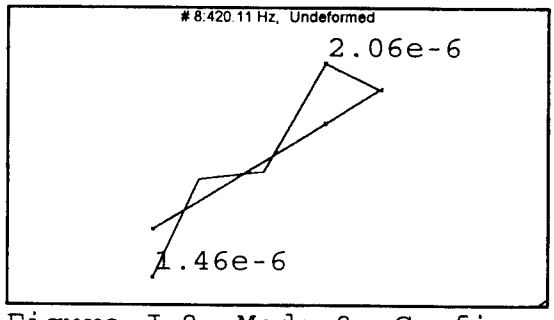

Figure J-8. Mode 8, Config 3.

MODE	Accelerometer Location	Amplitude	Phase Angle
1	1	71.72e-6	-80.78
	2	189.52e-6	-84.06
	3	354.27e-6	-84.88
	4	506.53e-6	-85.80
	5	556.14e-6	-86.72
2	1	1.96e-6	54.40
	2	36.23e-6	-82.86
	3	39.25e-6	-175.53
	4	34.82e-6	132.15
	5	46.26e-6	135.08
3	1	5.62e-6	127.16
	2	12.63e-6	118.70
	3	2.08e-6	129.75
	4	8.98e-6	18.42
	5	13.42e-6	-36.35
4	1	1.24e-6	-52.19
	2	2.18e-6	127.41
	3	3.76e-6	142.48
	4	913.02e-9	-25.75
	5	1.87e-6	-51.40
5	1	2.54e-6	-36.48
	2	1.10e-6	-78.49
	3	6.96e-6	140.39
	4	3.22e-6	-137.80
	5	6.49e-6	-33.26

Table J-1. Amplitudes and phases computed by STARModal for configuration 3.

MODE	Accelerometer Location	Amplitude	Phase Angle
6	1	251.40e-9	13.72
	2	1.71e-6	-103.38
	3	1.79e-6	77.45
	4	45.15e-9	-40.94
	5	2.41e-6	-88.78
7	1	1.35e-6	166.90
	2	50.07e-9	-148.66
	3	20.50e-9	-152.46
	4	308.65e-9	160.57
	5	2.41e-6	37.57
8	1	678.70e-9	-167.51
	2	2.06e-6	104.21
	3	344.72e-9	-118.00
	4	701.30e-9	86.12
	5	1.46e-6	-80.51

Table J-1 (cont.).

APPENDIX K. MODAL SHAPES FOR CONFIGURATION 4

Gun configuration 4 had the uppermost barrel in firing position, no muzzle restraint, and a static load pulling back on the stub rotor to simulate the maximum load experienced during firing.

STARModal identified eight modes (Figures K-1 to K-8) in the 2-500 Hz excitation range for this configuration. The numbers on the shapes are relative displacements between the corresponding points on the shape. No other connotation should be attributed to them.

Table K-1 lists the amplitudes and phase angles computed by STARModal for configuration 4.

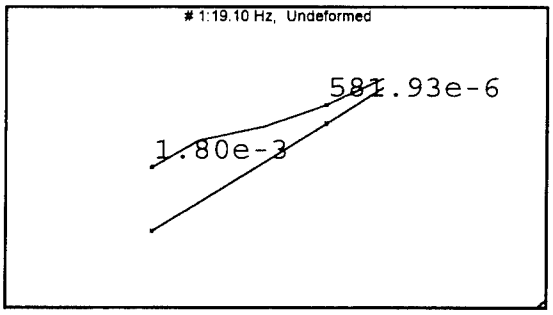

Figure K-1. Mode 1, Config 4.

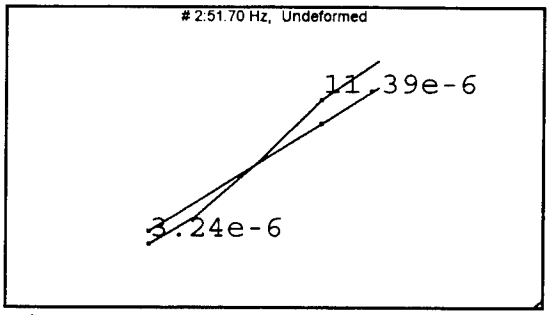

Figure K-2. Mode 2, Config 4.

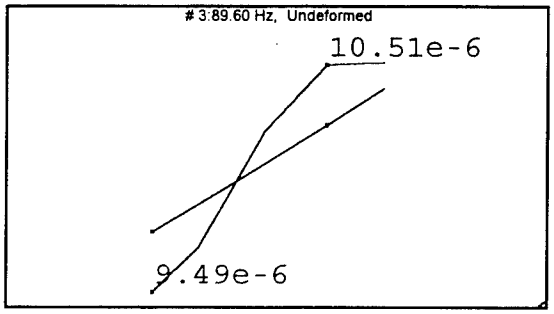

Figure K-3. Mode 3, Config 4.

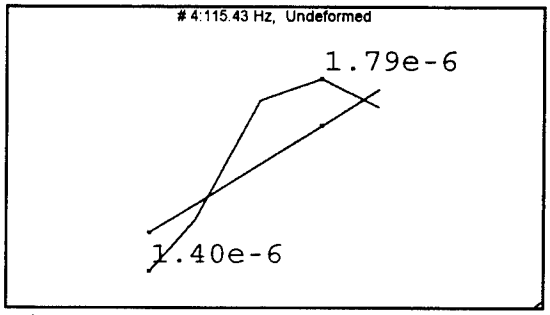

Figure K-4. Mode 4, Config 4.

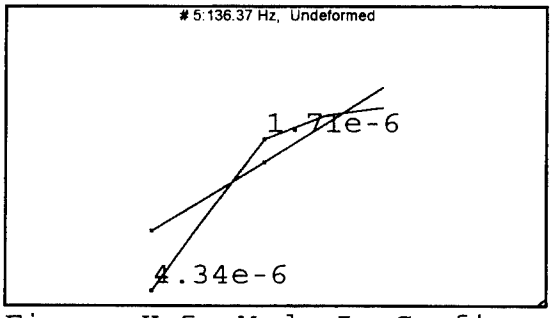

Figure K-5. Mode 5, Config 4.

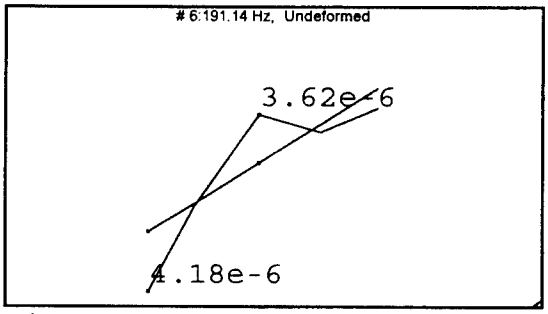

Figure K-6. Mode 6, Config 4.

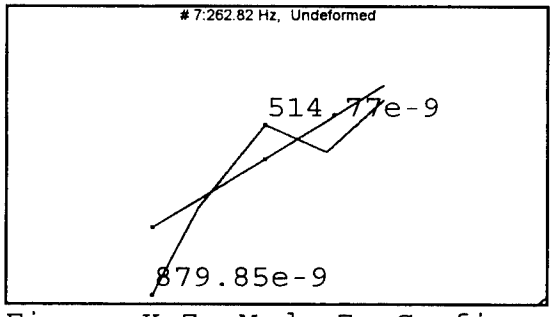

Figure K-7. Mode 7, Config 4.

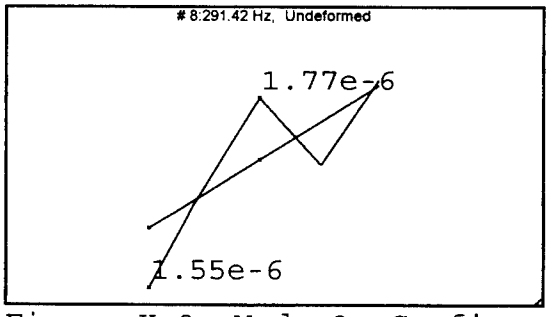

Figure K-8. Mode 8, Config 4.

MODE	Accelerometer Location	Amplitude	Phase Angle
1	1	289.80e-6	-13.26
	2	581.93e-6	-25.36
	3	1.03e-3	-20.85
	4	1.74e-3	1.17
	5	1.80e-3	9.82
2	1	5.42e-6	126.93
	2	11.39e-6	-167.94
	3	1.71e-6	-158.86
	4	4.88e-6	-119.10
	5	3.24e-6	-110.38
3	1	4.90e-6	122.83
	2	10.51e-6	122.76
	3	5.62e-6	121.10
	4	7.31e-6	-60.24
	5	9.49e-6	-58.22
4	1	902.28e-9	-9.41
	2	1.79e-6	121.15
	3	2.39e-6	118.86
	4	535.59e-9	-38.26
	5	1.40e-6	-40.04
5	1	1.47e-6	-42.80
	2	746.50e-9	131.61
	3	1.71e-6	138.26
	4	1.73e-6	-52.18
	5	4.34e-6	-46.43

Table K-1. Amplitudes and phases computed by STARModal for configuration 4.

MODE	Accelerometer Location	Amplitude	Phase Angle
6	1	1.55e-6	-42.29
	2	585.81e-9	-46.29
	3	3.62e-6	140.29
	4	141.12e-9	31.08
	5	4.18e-6	-39.49
7	1	205.18e-9	-18.16
	2	447.08e-9	-28.05
	3	514.77e-9	142.56
	4	145.88e-9	36.38
	5	879.85e-9	-25.13
8	1	174.74e-9	144.52
	2	1.26e-6	-23.19
	3	1.77e-6	153.25
	4	54.15e-9	1.31
	5	1.55e-6	-25.40

Table K-1 (cont.).

APPENDIX L. MODAL SHAPES FOR CONFIGURATION 5

Gun configuration 5 had the uppermost barrel in firing position, the current U.S. Navy deployed muzzle restraint attached, and a static load pulling back on the stub rotor to simulate the maximum load experienced during firing.

STARModal identified thirteen modes (Figures 4-12 to 4-24 in Chapter IV) in the 2-500Hz excitation range for this configuration. The numbers on the shapes are relative displacements between the corresponding points on the shape. No other connotation should be attributed to them.

Table L-1 lists the amnplitudes and phase angles computed by STARModal for configuration 5.

MODE	Accelerometer Location	Amplitude	Phase Angle
1	1	35.37e-6	-86.62
	2	79.69e-6	-63.09
	3	122.83e-6	-54.20
	4	163.08e-6	-40.53
	5	191.33e-6	-25.19
2	1	1.49e-6	119.39
	2	2.65e-6	123.62
	3	616.26e-9	-163.25
	4	2.43e-6	-31.41
	5	2.16e-6	-52.99
3	1	20.23e-9	-7.25
	2	470.63e-9	142.83
	3	2.35e-6	179.78
	4	161.93e-9	-161.40
	5	332.72e-9	-53.99
4	1	2.26e-6	69.24
	2	572.54e-9	122.89
	3	1.41e-6	72.58
	4	839.58e-9	131.76
	5	365.63e-9	32.28
5	1	122.59e-9	-84.41
	2	227.38e-9	121.83
	3	455.87e-9	104.71
	4	101.66e-9	64.66
	5	315.77e-9	-72.87

Table L-1. Amplitudes and phases computed by STARModal for configuration 5.

MODE	Accelerometer Location	Amplitude	Phase Angle
6	1	197.81e-9	-55.87
	2	1.59e-6	128.67
	3	202.30e-9	18.11
	4	3.34e-6	-51.54
	5	5.94e-6	-45.71
7	1	1.63e-6	-34.70
	2	615.15e-9	-52.05
	3	4.39e-6	-143.49
	4	548.69e-9	27.32
	5	5.62e-6	-38.83
8	1	1.74e-6	-37.11
	2	362.88e-9	-55.54
	3	4.20e-6	122.70
	4	65.39e-9	-120.59
	5	2.84e-6	-58.76
9	1	224.50e-9	8.07
	2	322.67e-9	-28.26
	3	1.75e-6	-113.51
	4	75.55e-9	88.17
	5	530.24e-9	-19.45
10	1	213.09e-9	137.16
	2	1.24e-6	-32.03
	3	1.59e-6	154.52
	4	37.91e-9	85.61
	5	1.61e-6	-42.16

Table L-1 (cont.).

MODE	Accelerometer Location	Amplitude	Phase Angle
11	1	267.43e-9	52.01
	2	503.44e-9	-114.64
	3	468.39e-9	43.72
	4	84.99e-9	-139.17
	5	99.69e-9	170.73
12	1	243.21e-9	146.02
	2	92.54e-9	-161.62
	3	247.38e-9	-59.17
	4	140.72e-9	83.08
	5	304.27e-9	-9.49
13	1	8.34e-9	-58.99
	2	33.52e-9	-144.59
	3	27.54e-9	4.45
	4	44.67e-9	-111.70
	5	21.50e-9	173.52

Table L-1 (cont.).

APPENDIX M. PCB 353B44 ACCELEROMETER CALIBRATION

Calibration sheet for the PCB Series 353 quartz shear mode accelerometer used to measure barrel assembly response to excitation. The use of shear mode quartz sensors reduces sensitivity to environmental effects that might bias the results.

Calibration Certificate

Per ISA-RP37.2

NPS Physics Acoustics Lab

Model No. 353B44

Serial No. 8006

PO No. _____ Customer _____

Calibration traceable to NIST thru Project No. 822/251101-93

ICP® ACCELEROMETER

with built-in electronics

Calibration procedure is in compliance with MIL-STD-45662A and traceable to NIST.

CALIBRATION DATA

Voltage Sensitivity	294.0	mV/g
Transverse Sensitivity	0.5	%
Resonant Frequency	18.5	kHz
Time Constant	1.0	s
Output Bias Level	9.9	V

KEY SPECIFICATIONS

Range	17	± g
Resolution	0.0005	g
Temp. Range	-65/+250	°F

METRIC CONVERSIONS:
ms⁻² = 0.102 g
°C = 5/9 x (°F -32)

90

Reference Frec

Frequency Hz	10	15	30	50	100	300	500	1000	2000			
Amplitude Deviation %	-.4	-.8	0.0	-.4	0.0	.1	.5	.8	1.8			

FREQUENCY RESPONSE

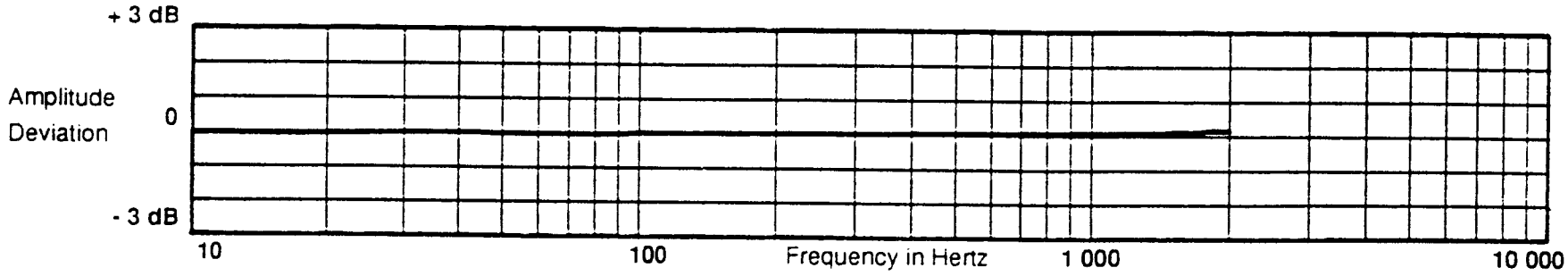

PCB

Piezotronics, Inc. 3425 Walden Avenue Depew, NY 14043-2495 USA

716-684-0001

Date 11/15/93

Calibrated by Ron Burke

APPENDIX N. BRÜEL AND KJÆR TYPE 8001 IMPEDANCE HEAD CALIBRATION

Calibration sheet for the B&K Type 8001 impedance head used to measure the force to the driving point.

Calibration Chart for Impedance Head Type 8001

Brüel & Kjær

Serial No. 1439315

Reference Sensitivity at 159.2 **Hz at** 23 °C **and including**

Cable Capacitance of 110 pF

Accelerometer:

Charge Sensitivity:**

3.25 pC/ms^{-2} or 31.9 pC/g*

Voltage Sensitivity:**

3.08 mV/ms^{-2} or 30.2 mV/g*

Capacitance (including cable) 1056 pF

Maximum Transverse Sensitivity at 30 Hz 1.8 %
For Resonant Frequency mounted on steel exciter of 180 grams and for Frequency Response of Force Gauge relative to Reference Sensitivity with impedance head acceleration constant, see attached individual Frequency Response Curve

Polarity is negative on the center of the accelerometer connector for an acceleration directed from the mounting surface into the body of the impedance head

Date 88 06 07 Signature

* 1 g = 9.807 ms^{-2} $\frac{mV}{g} = \frac{mV_{RMS}}{g_{RMS}} = \frac{mV_{peak}}{g_{peak}}$

** This calibration is traceable to the National Bureau of Standards Washington D C

0058 12

Force Gauge:

Charge Sensitivity 315 pC/N

Voltage Sensitivity 344 mV/N

Capacitance (including cable) 799 pF

Base Strain Sensitivity of Force Gauge: 3 × 10^{-4} N/μStrain

Stiffness below Accelerometer: 25 × 10^{7} N/m

Mass below Force Gauge: 2.2 gram

Max. Screw-Down Torque: 0.5 Nm

Physical:

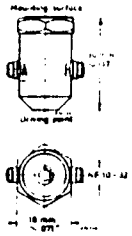

Weight: 51 gram
Material:
Titanium & Stainless Steel
Mounting Thread:
10 - 32 UNF-2B
Electrical Connector:
Miniature coaxial
10 - 32 UNF-2A thread

ACOUSTICS-BAKER
Code 618a
NPS Physics Dept.

Environmental:

Humidity: Sealed
Max. Temperature: 260°C or 500°F
Magnetic Sensitivity (50 Hz): < 20 mV/T
Acoustic Sensitivity:
< 0.003 ms^{-2} or 0.03 g at 154 dB SPL
Resistance min. 20 000 mΩ at room temperature.

For further information see instruction book

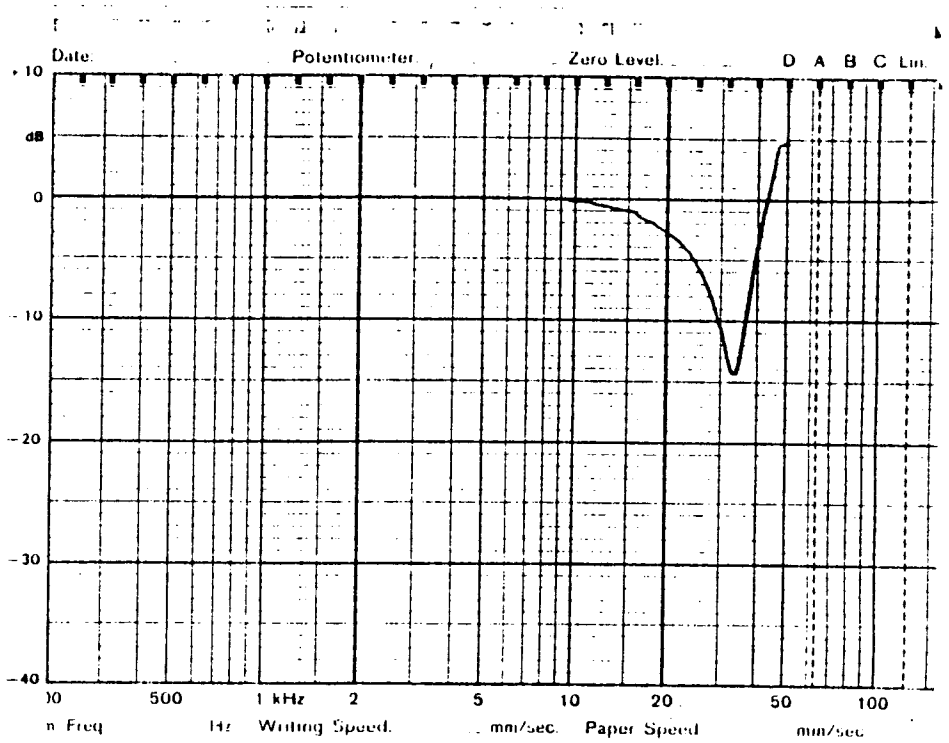

LIST OF REFERENCES

1. NAVAIR 11-95M61A1-1, *Maintenance Instructions with Illustrated Parts Breakdown Intermediate Level, M61A1 20mm Automatic Gun*, Commander, Naval Air Systems Command, 1990.

2. NAVSEA OP 4154 Volume 1, Part 1, *Close-in Weapon System Mk 15 Mods 1 thru 4 and 6 (PHALANX)*, Commander, Naval Sea Systems Command, 1987.

3. Macneil, Donald P., *Normal Modes of Oscillation of The Vulcan PHALANX Close-in Weapons System*, Naval Postgraduate School Master's Degree Thesis, June, 1993.

4. Peterschmidt, John C., *Normal Modes of Vibration of the PHALANX Gun*, Naval Postgraduate School Master's Degree Thesis, June, 1993.

5. APS Dynamics (Acoustics Power Systems), Carlsbad, California,(619)438-4848.

6. Brüel and Kjær, Anaheim, California, (714)978-8066.

7. Hewlett-Packard, Palo Alto, California, (415)968-9200.

8. PCB Piezotronics, Inc, Depew, New York, (716)684-0001.

9. Døssing, Ole, *Structural Testing* (Parts 1 and 2), Brüel and Kjær, 1988.

10. Thomson, William T., *Theory of Vibrations with Applications*, Prentice Hall, 1988.

11. Structural Measurement Systems, Milpitas, California, (408)432-8600.

12. Structural Measurement Systems, *STAR Reference Manual*, Structural Measurement Systems, 1990.

13. Kinsler, Lawrence E., Austin R. Frey, Alan B. Coppens, and James V. Sanders, *Fundamentals of Acoustics*, John Wiley and Sons, 1982.

14. Cela, David, *Correlation of Bullet Dispersion and Transverse Barrel Tip Displacement Data Measured on a Firing PHALANX Gun System*, Naval Postgraduate School Master's Degree Thesis, Monterey, CA, December, 1994.

INITIAL DISTRIBUTION LIST

1. Defense Technical Information Center — 2
   Cameron Station
   Alexandria, Virginia 22304-6145

2. Library, Code 52 — 2
   Naval Postgraduate School
   Monterey, California 93943-5101

3. Professor William B. Colson Code PH/Cw — 2
   Chairman, Department of Physics
   Naval Postgraduate School
   Monterey, California 93943-5000

4. Professor Steven R. Baker Code PH/Ba — 2
   Department of Physics
   Naval Postgraduate School
   Monterey, California 93943-5000

5. Yuji Wilson — 1
   Port Hueneme Division
   Naval Surface Warfare Center
   Code 4121
   Port Hueneme, California 93043

6. Mike Hatch — 1
   2163 Woodleaf Way
   Mountain View, California 94040

7. Lt David Cela — 1
   29 Fairlawn Street
   Ho-Ho-Kus, New Jersey 07431

8. Capt Robert J. Hansberry — 2
   USMC Systems Command
   2033 Barnett Ave., Suite 315
   Quantico, Virginia 22134-5010

9. Director, Training and Education — 1
   MCCDC, Code C46
   1019 Elliot Rd.
   Quantico, Virginia 22134-5027